Three-dimensional display technologies of recent interest: principles, status, and issues [Invited]◇

Jisoo Hong,[1] Youngmin Kim,[1] Hee-Jin Choi,[2] Joonku Hahn,[3] Jae-Hyeung Park,[4] Hwi Kim,[5] Sung-Wook Min,[6] Ni Chen,[1] and Byoungho Lee[1,*]

[1]School of Electrical Engineering, Seoul National University, Gwanak-Gu Gwanakro 1, Seoul 151-744, South Korea

[2]Department of Physics, Sejong University, 98 Gunja-Dong, Gwangjin-Gu, Seoul 143-747, South Korea

[3]School of Electronics Engineering, Kyungpook National University, 1370 Sankyuk-dong, Buk-gu, Daegu 702-701, South Korea

[4]School of Electrical & Computer Engineering, Chungbuk National University, Heungduk-Gu, Cheongju-Si, Chungbuk 361-763, South Korea

[5]Department of Electronics and Information Engineering, College of Science and Technology, Sejong Campus, Korea University, Jochiwon-eup, Yeongi-gun, Chungnam 339-700, South Korea

[6]Department of Information Display, Kyung Hee University, Dongdaemoon-ku, Seoul 130-701, South Korea

*Corresponding author: byoungho@snu.ac.kr

Recent trends in three-dimensional (3D) display technologies are very interesting in that both old-fashioned and up-to-date technologies are being actively investigated together. The release of the first commercially successful 3D display product raised new research topics in stereoscopic display. Autostereoscopic display renders a ray field of a 3D image, whereas holography replicates a wave field of it. Many investigations have been conducted on the next candidates for commercial products to resolve existing limitations. Up-to-date see-through 3D display is a concept close to the ultimate goal of presenting seamless virtual images. Although it is still far from practical use, many efforts have been made to resolve issues such as occlusion problems.   © 2011 Optical Society of America

OCIS codes: 110.2990, 100.6890.

◇**Datasets associated with this article are available at** http://hdl.handle.net/10376/1596. **Links such as "View 1" that appear in figure captions and elsewhere will launch custom data views if ISP software is present.**

1.   Introduction

Three-dimensional (3D) display has a long history, starting from the first suggestion of a stereoscope by Wheatstone in the mid-19th century [1] through active inventions of various autostereoscopic technologies in the late 19th and early 20th centuries, an era of holography in the 1960s and 1970s, and the adoption of digital devices today. Although most of the basic ideas were proposed more than tens of years ago or even 100 years ago, none of them are without critical issues that are obstacles to catching a mass market. Since the late 1990s, development in digital devices has led to widespread use of flat panel displays (FPDs), especially those based on liquid crystal (LC) technology. It was a catalyst for research on implementing commercially acceptable 3D

displays again. From Fig. 1, recent research trends in 3D display can be inferred. It is interesting to see that research on autostereoscopic displays, including parallax barriers, integral imaging, and lenticular lenses, has grown continuously, starting from around the year 2000, when LC displays (LCDs) became popular. In particular, the parallax barrier, which is more suitable for implementation with LCDs, shows a steeper increase compared with other autostereoscopic technologies. Despite increasing research interest and demand from the market, up until a few years ago, it was a major opinion that 3D display was still far from mass commercialization.

The past few years will be marked as a "historic" period in 3D display technology because, for the first time, several major manufacturers in the display industry have started to supply successful commercial products based on stereoscopy to the mass market. Stereoscopy is a technology that has a history of more than 170 years and there have been no notable breakthroughs other than research and inventions conducted in its early decades. The only difference in the circumstance is that a value chain of the industry started to work with 3D films, which became common and popular in ordinary theaters after the success of the monumental movie "Avatar." Commercialization revealed new issues of stereoscopy in the aspect of products and 3D has again become a very active research topic. The current research trends in the field of 3D display are very interesting: old-fashioned technologies, such as stereoscopy and science fiction movielike fancy technologies, are active and popular research topics together. This phenomenon comes from a larger time lag of commercialization to the latest technologies compared with other industries. In this tutorial paper, recent research interest in 3D display will be outlined, covering both product-focused and up-to-date technologies.

2. Depth Cues in Perceiving 3D Images

The human visual system (HVS) perceives the 3D information of an input image by various depth (or distance) cues, which can be categorized as psychological and physiological cues. Psychological cues are associated with a process inside the brain to analyze visual information based on learned experiences. The HVS can infer rough 3D information from even a two-dimensional (2D) image, such as an ordinary photograph, with psychological cues if it does not include artificial contradictions or ambiguous relationships. In contrast, physiological cues are information related to a physical reaction of the human body when a 3D image is given to the HVS. Physiological cues can provide more exact 3D information without ambiguity. The objective of 3D display is to reproduce 3D images by using various depth cues to stimulate the HVS.

Psychological cues include linear perspective, overlapping, shading, and texture gradients. These representative psychological cues are described in Fig. 2(a) and they are learned through everyday life. Of course, they are not all of the psychological cues, but countless empirical data is also used to analyze an image. However, such an image-based approach always involves ambiguities and errors because it cannot provide complete real depth information. With only psychological cues, one forms an understanding of 3D information rather than feeling it. Because of such ambiguities and errors, investigations on extracting depth information from a single 2D image based on psychological cues does not yet show satisfactory results. If a display system is to be categorized as 3D display, it should provide not only psychological but also physiological depth cues.

Figure 2(b) briefly describes reactions of the human body related to a series of physiological depth cues. Binocular disparity or stereopsis, which is most prominent among the physiological depth cues, is acquiring depth information from the parallax appearing in two images obtained from the left and right eyes. Because it gives most of the 3D information that can be obtained from physiological cues, early 3D displays were based on a binocular disparity. Stereoscopic or autostereoscopic displays are categories that use only binocular disparity from among the physiological depth cues. Actually, the term "autostereoscopic display" itself only means that it can give stereopsis without any special apparatus and, hence, it does not imply a restriction to other physiological cues. However, it is usual to classify 3D displays with other physiological cues as volumetric displays. Although stereoscopic or autostereoscopic displays provide sufficient 3D information to observers, visual fatigue or discomfort has always been a challenging issue in using them as commercial 3D displays. It is still unclear what really causes the discomfort, but researchers believe that conflicts
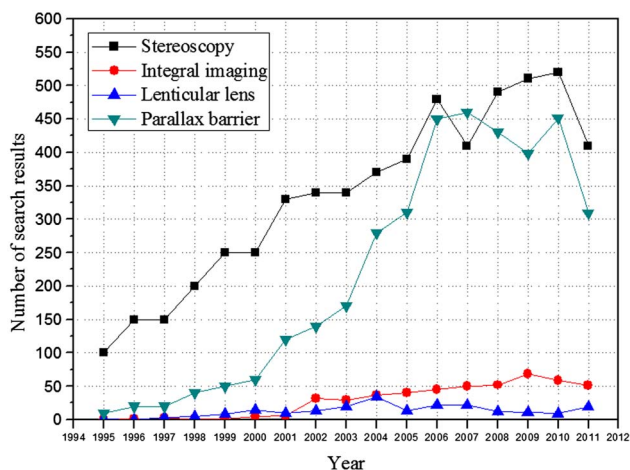

Fig. 1. (Color online) Number of search results from Google Scholar (http://scholar.google.com). Searching was restricted only to titles of papers. Queries for each technology were "stereoscopy or stereoscopic," "integral imaging," "lenticular lens," and "parallax barrier.". Numbers in 2011 are estimations based on the results obtained on July 2011.
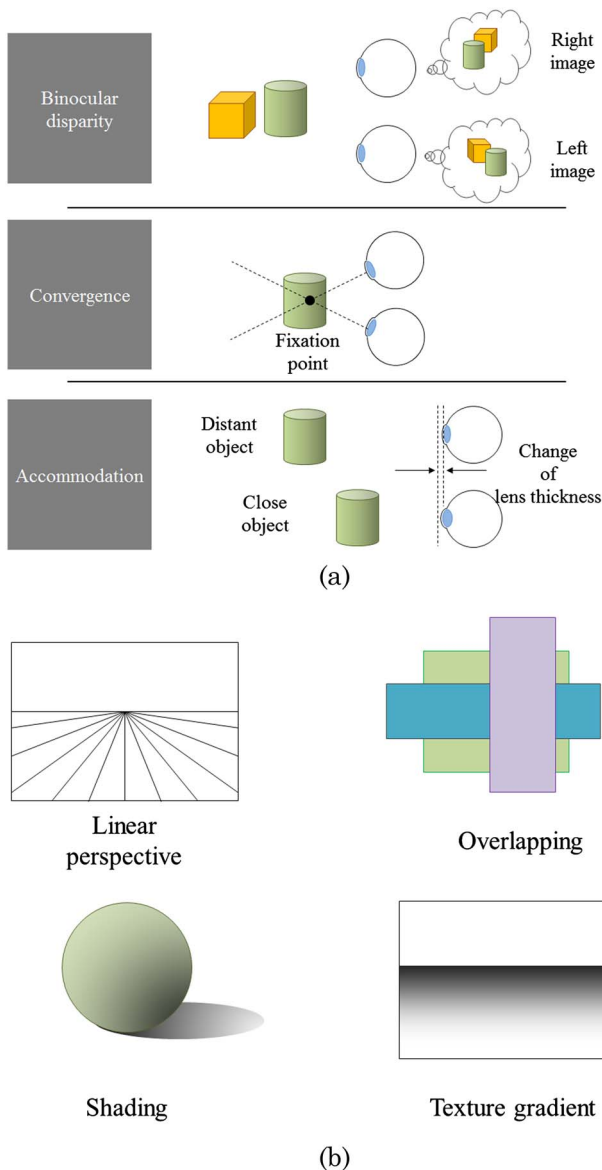
Fig. 2. (Color online) Depth cues associated with 3D information: (a) psychological cues and (b) physiological cues.

between the information obtained from artificially produced cues may be a reason. There are other physiological cues, such as ocular convergence and accommodation, as shown in Fig. 2(b). Ocular convergence is a reaction that involves rotating the ocular globes to create a fixation point at a location of the 3D object of interest. Accommodation is to control an eye lens to make a clear image of the 3D object on the retina. In stereoscopic or autostereoscopic displays, convergence is usually satisfied, while accommodation never is because the images are in focus on the display. It is believed that such a conflict can be a source of visual fatigue [2]. Other than such an accommodation–convergence mismatch, error in vertical disparity and crosstalk between left and right images can disturb the stereoscopic relationship and they can be other reasons for visual fatigue [3]. Many investigations have been conducted to

reduce or eliminate such issues in stereoscopic or autostereoscopic displays; however, there is no definite solution yet. Volumetric display and holographic display are approaches to resolving such issues by providing all of the physiological depth cues. Although it is a definite way to deal with visual fatigue, it requires a huge amount of information in implementation. Hence, it is more of a future technique in a road map of 3D display.

3. Stereoscopic 3D Display Technologies

Stereoscopic 3D display technologies use special glasses to induce binocular disparity and convergence by providing different left-eye and right-eye images to the observer. Generally, they are categorized according to the types of the glasses—LC shutter glasses and polarization glasses. Recently, with the improvements of FPD technologies, stereoscopic 3D display was able to reach the level of commercialization and several stereoscopic 3D products are on sale in the market. One of the most advantageous features of those stereoscopic 3D products is that they can be made using the existing FPD manufacturing processes and, therefore, require little additional cost. As a result, stereoscopic 3D products are regarded as an important step in the advance of the popularization of 3D display technologies. By now, there are three stereoscopic 3D display technologies adopted or to be adopted in 3D monitors and TVs. Among them, one requires LC shutter glasses, while the others need polarization glasses and polarization modulators for the additional 3D devices. In this section, the basic principles and structures of the above three technologies will be reviewed and their pros and cons will be compared. Although stereoscopic 3D display can be realized using an LCD, a plasma display panel, or an organic light-emitting diode (OLED) display, the review in this section is based on the case of stereoscopic 3D LCD since most of the stereoscopic 3D products use LCD panels as display devices.

The first one to review is a 3D technology with LC shutter glasses. The LC shutter glasses are composed of two active LC shutters that can open and block the observer's left eye and right eye separately. With the operation of LC shutters, the glasses can make the observer watch images displayed on the display panel only through the left eye or the right eye. As a result, if the display panel shows the left-eye and the right-eye images in different frames in a manner synchronized with the operation of the LC shutter glasses, the observer may feel the binocular disparity and convergence from the recognized images. For realizing a stereoscopic 3D display with the above principle, a display device with a frame rate higher than 120 or 240 Hz, a wireless protocol for connection and synchronization of the LC shutter glasses with the display device, and a technology for a fast LC shutter are required. These devices are already commercialized. Therefore, it is possible to realize a 3D display with LC shutter glasses with

minimum additional cost. However, there are some factors to be regarded in arranging the left-eye and the right-eye images in different image frames. In the case of using an LCD panel as a display device, the left-eye and the right-eye images are switched in a line-by-line sequence (progressive scan). Hence, a separation frame is required between the left-eye and the right-eye image frames. As an image of the separation frame, a black image is commonly used and an additional backlight operation, such as scanning or blinking, can be added to enhance the quality of 3D images. Figure 3 shows the principle of stereoscopic 3D display with LC shutter glasses using a 240 Hz LCD panel with a sequence of left-eye image frame → black frame → right-eye image frame → black frame (LBRB) operation and an additional backlight operation [4,5].

Since the left-eye and right-eye images are displayed in different frames using all pixels in the display device, the 3D technology using the LC shutter glasses has no resolution degradation in displaying 3D images. In other words, current 3D monitors or TVs using LC shutter glasses can realize full-high-definition (full-HD, 1920 × 1080 pixels) 2D and 3D images. Since the resolution is one of the key factors of image quality, the 3D technology using LC shutter glasses has an advantage in this respect. Moreover, LBRB operation can be adopted by a minor revision of the image processing unit in the 2D LCD module. As a result, the 3D technology with LC shutter glasses requires a minimum level of change in the structure of the 2D LCD module and has become the most practical solution for 3D products. However, the technology also has some issues to be improved. First, due to the inserted black image frames and the shuttering operation in the glasses, the luminance of the 3D image reduces to lower than a quarter of that of the 2D image. Second, in the case of slow LC response, a residual image of the black image (no image) frame can remain and become a cause of 3D crosstalk, i.e., the overlapping of the left-eye and the right-eye images. The backlight operation, such as scanning or blinking, is to prevent the 3D crosstalk by compensating the incomplete response of the LC. The last issue is that the weight and the price of LC shutter glasses are higher than those of polarization glasses due to the adoption of electronic devices. Therefore, researchers are trying to make progress
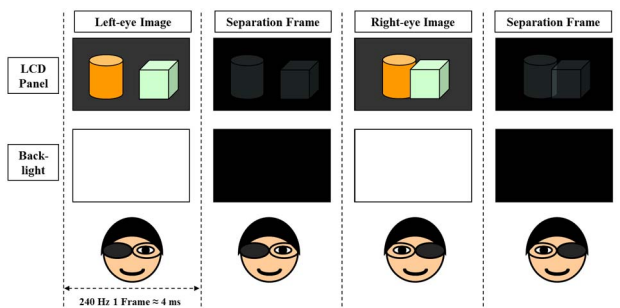
on the above issues and, recently, a 3D TV with LC shutter glasses and 240 Hz ultrahigh-definition (UHD, 3840 × 2160) LCD panel was exhibited in Display Week 2011 by Samsung Electronics.

The next two stereoscopic 3D display technologies use polarization glasses to induce binocular disparity and convergence. The basic principle of those methods is to adopt a polarization modulator in the display device to make the left-eye and right-eye images have orthogonal polarization to each other. Therefore, polarization glasses are composed of two polarization filters to separate the left-eye and the right-eye images with orthogonal polarizations. In modulating the polarization of the left-eye and the right-eye images, there are two different methods—spatial modulation and frame modulation. The former one is called a patterned retarder (PR), while the latter is known as an active retarder (AR) or shutter in panel (SIP). The principle of the PR method is to display an interleaved mixture of the left-eye and the right-eye images and to impose the polarization of them using a PR. Since the LCD panel itself has a linear polarizer on its top (front) surface, it is possible to make the left-eye and right-eye images have left-handed and right-handed circular polarizations by inducing phase retardations with π difference. Since it is common to arrange the left-eye and right-eye images to have only odd or even pixel lines (line-by-line arrangement), the PR needs to have same structure and to be aligned with high accuracy to prevent 3D crosstalk. Figure 4 shows the structure and principle of the PR technology [6].

In the example of Fig. 4, the LCD panel is assumed to have eight pixel lines and the left-eye and right-eye images have four pixel lines each. However, for current 3D TV with PR technology, an LCD panel with full-HD resolution is commonly used and the number of pixel lines for each eye's image is 540. The PR method does not need to insert the black image frame and the luminance of the 3D image is almost 2 times higher than that of the 3D technology with LC shutter glasses. Moreover, the slow response

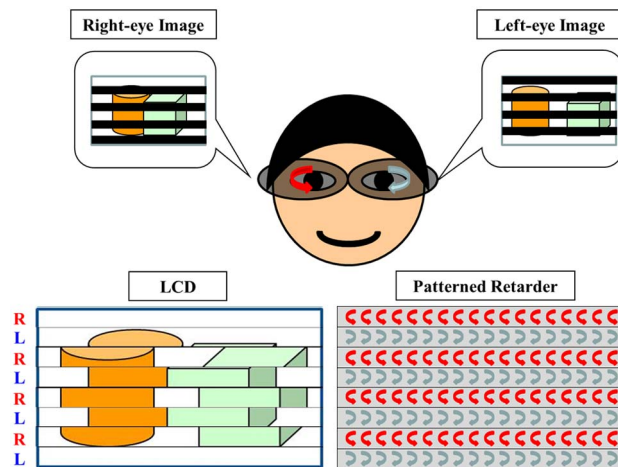Fig. 3. (Color online) Principle of stereoscopic 3D display with LC shutter glasses.

Fig. 4. (Color online) Structure and principle of PR technology.

of LC does not affect the 3D crosstalk since the left-eye and right-eye images are displayed in a single frame. The use of lighter and cheaper polarization glasses is another attractive point and the use of circular polarization to separate the images allows the observers to rotate their heads without a concern of luminance degradation. In spite of those advantages, the early models of PR technology used a glass PR filter with a high manufacturing cost and resulted in only a small volume of sales. This year, with a new technology (by LG Display) to replace the glass PR with a film PR (FPR), the manufacturing cost of FPR 3D TVs was considerably reduced and the price of them is now lower than 3D TVs with LC shutter glasses, while the above advantages are conserved.

The 3D resolution of the FPR method is still under discussion. Although it is clear that the left-eye and right-eye images have half numbers of pixel lines, there are two opinions in opposite positions. The first one is that the 3D resolution of FPR 3D TV is the same as that of the left-eye and right-eye images and is only half of 2D resolution. In other words, an FPR 3D TV with a full-HD LCD panel has half of the full-HD 3D resolution with 540 pixel lines. The manufacturer of 3D displays with LC shutter glasses supports this opinion. In contrast, the manufacturer of FPR 3D displays is claiming that the 3D image recognition is done by a combination of the left-eye and right-eye images and, therefore, has full-HD resolution with 1080 pixel lines. A demonstration was proposed by the FPR manufacturer to count the number of lines by moving the 3D image by one line each time, and the result was that 1080 movements were counted. Several organizations, such as Interteck and the 3rd Institute in China and Verband Deutscher Elektrotechniker in Germany have verified the above demonstration, while another organization, Consumer Reports in the USA, is on the negative side about it, even though it listed the FPR 3D TV at the No. 1 position in a performance test among the 3D TVs sold in the USA.

The last stereoscopic 3D display technology, which is called AR or SIP, requires passive polarization glasses but a time-sequential polarization modulator. The basic principle of AR or SIP technology is to display the left-eye and right-eye images in different frames with orthogonal polarizations and those images are separated by polarization glasses [7]. For that purpose, the time-sequential polarization modulator needs to operate with a speed faster than 120 Hz and the display device has to be synchronized with it, as shown in Fig. 5.

With the structures and principles above, it can be thought that the polarization glasses and the AR have the same role as the LC shutter glasses. Therefore, the 3D TV using AR technology can provide a full-HD 3D image with almost the same luminance as that of the FPR method. However, similar to the case of LC shutter glasses, a special technique, such as black image frame insertion, may be required to synchronize the operation of AR with the switch-
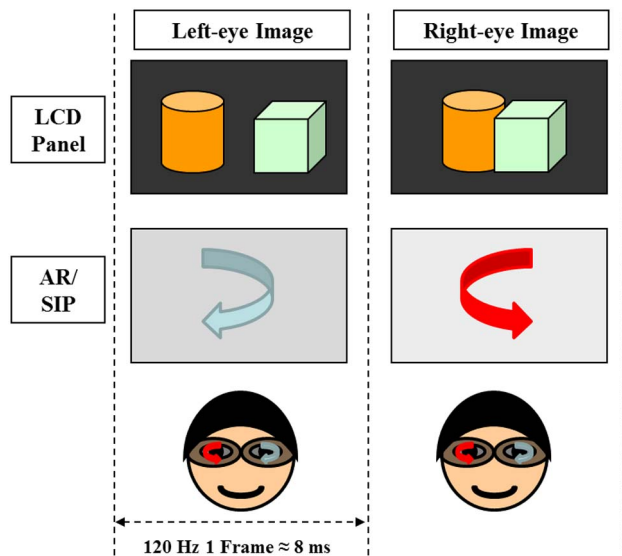

Fig. 5. (Color online) Structure and principle of AR or SIP technology.

ing of the left-eye and right-eye images because of the progressive scan, and the luminance of the 3D image may be reduced. Another weak point of the AR technology is that the manufacturing cost of AR or SIP itself is expected to be higher than others. Since the AR or SIP is also an active LCD panel with simpler structure, the 3D display with the AR method is actually composed of two LCD panels. Considering that the LCD panel is the most expensive part of an LCD module, it is not easy for the 3D display with AR technology to achieve a competitive price. However, there is continuous research on the AR or SIP technology for next-generation stereoscopic 3D products and, recently, a 3D notebook PC, a 3D monitor, and a 3D TV based on the SIP technique were exhibited at Display Week 2011 (May 2011, Los Angeles, California).

Although each of the above stereoscopic 3D display technologies has its own pros and cons, there are a common advantage and a common issue to be improved for all of them. As described above, the most advantageous point is that the stereoscopic 3D products can show a 3D image with high quality and low cost. However, the need to wear 3D glasses is a major concern no matter what kind of glasses they are. The NPD Group in the USA has announced that 42% of consumers who will not buy the 3D TV answered that the 3D glasses were not comfortable to them. Therefore, researchers in 3D technology are trying to realize a practical autostereoscopic (without using glasses) 3D display. The details of autostereoscopic 3D technology will be reviewed in the following sections.

4. Autostereoscopic 3D Display Technologies

A. Lenticular Lens

The lenticular lens technology is to attach a one-dimensional array of lenticular lenses to distribute

the pixels of the display device to multiple viewpoints. The role of a lenticular lens is to magnify and transfer the information of specific pixels to a designated position, as shown in Fig. 6. Therefore, observers in different viewpoints can watch different images, and binocular disparity, convergence, and motion parallax can be realized. However, since it is impossible for the observer to watch all pixels at once, the 3D resolution is reduced and there is a trade-off relation between the resolution of the 3D image and the number of viewpoints. In spite of the above weak point, the lenticular lens technique is expected to be suitable for early outdoor 3D digital signage because it can provide 3D images with high luminance.

Since it is obvious that the resolution of 3D image should be reduced in a lenticular lens system, there are two advanced techniques to compensate it. One of them is a slanted lenticular system to distribute the loss of resolution into both the horizontal and vertical directions by slanting the structure of the lenticular lens or rearranging the color filter of pixels [8]. The other is LC lens technology, which enables the lenticular lens display system to become a switchable 2D/3D display by electrically generating or eliminating the lenticular lens. In the early age, a refractive LC lens was commonly used for the above role. However, due to the problems that come from the thickness of the refractive LC lens, researchers are now trying to develop a practical diffractive LC lens [9–12]. Figure 7 shows the operation of a 2D/3D lenticular lens using the patterned electrode method recently developed by LG Electronics. The electric field at the part of the lens edge is much stronger than the electric field at the center of the lens. This nonuniform distribution of electric field causes nonuniform distribution of the tilt angle of the LC direc-
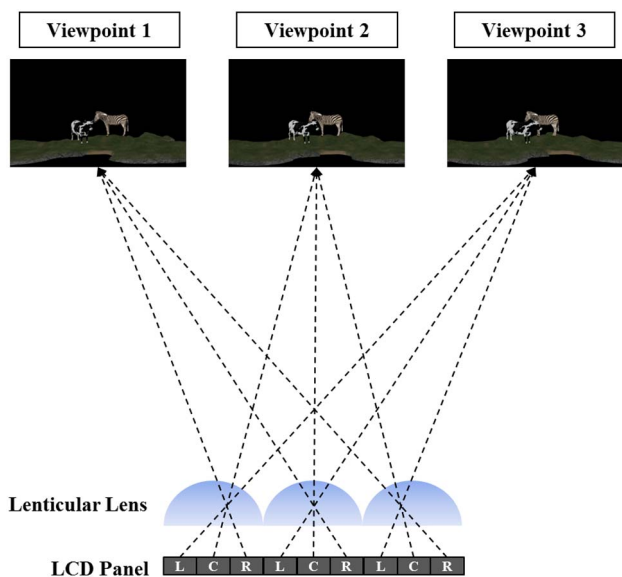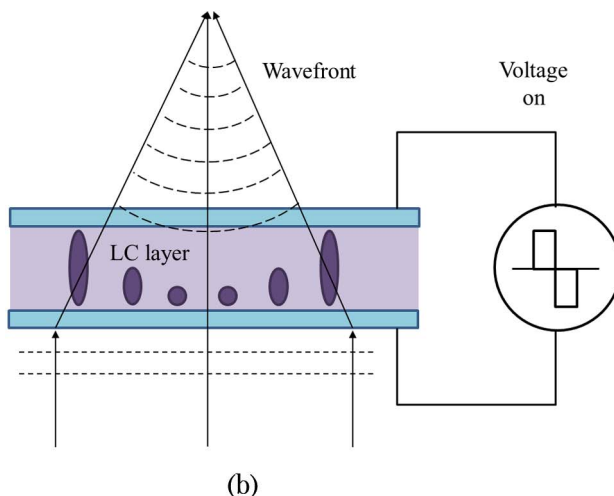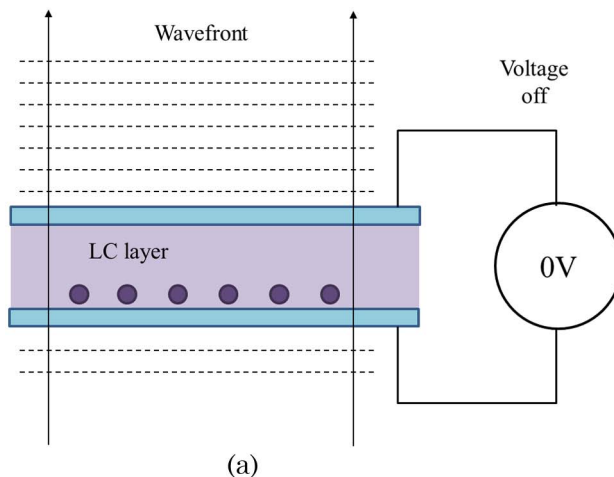

(a)

(b)

Fig. 7. (Color online) Operation of a 2D/3D convertible lenticular lens display using the patterned electrode method: (a) 3D mode and (b) 2D mode.

tor, and the refractive index distribution changes accordingly.

B. Parallax Barrier

A parallax barrier is very similar to the lenticular lens in the fundamental principle of showing 3D images. Instead of using a lenticular lens sheet, a parallax barrier adopts an array of vertical masks to show different views to the left and right eyes. As shown in Fig. 8(a), if an array of vertical masks (or slits) was properly designed, there would be a certain viewing position where each eye could see only even or odd columns of pixels through slits between masks. Hence, the left and right eyes would watch different images composed of only even or odd columns of pixels, which stimulates stereopsis. A parallax barrier setup can be easily extended to a multiview case by expanding the size of each mask. Roughly, an array of vertical masks whose mask pitch is n times larger than the pixel pitch of the display panel gives n views. A parallax barrier has the same resolution reduction problem as a lenticular

Fig. 6. (Color online) Principle and structure of a three-view lenticular lens 3D display.

Viewpoint 1 Viewpoint 2

Parallax
barrier

LCD
panel

L R L R L R L R

(a)

2D mode

2D image

Parallax
barrier
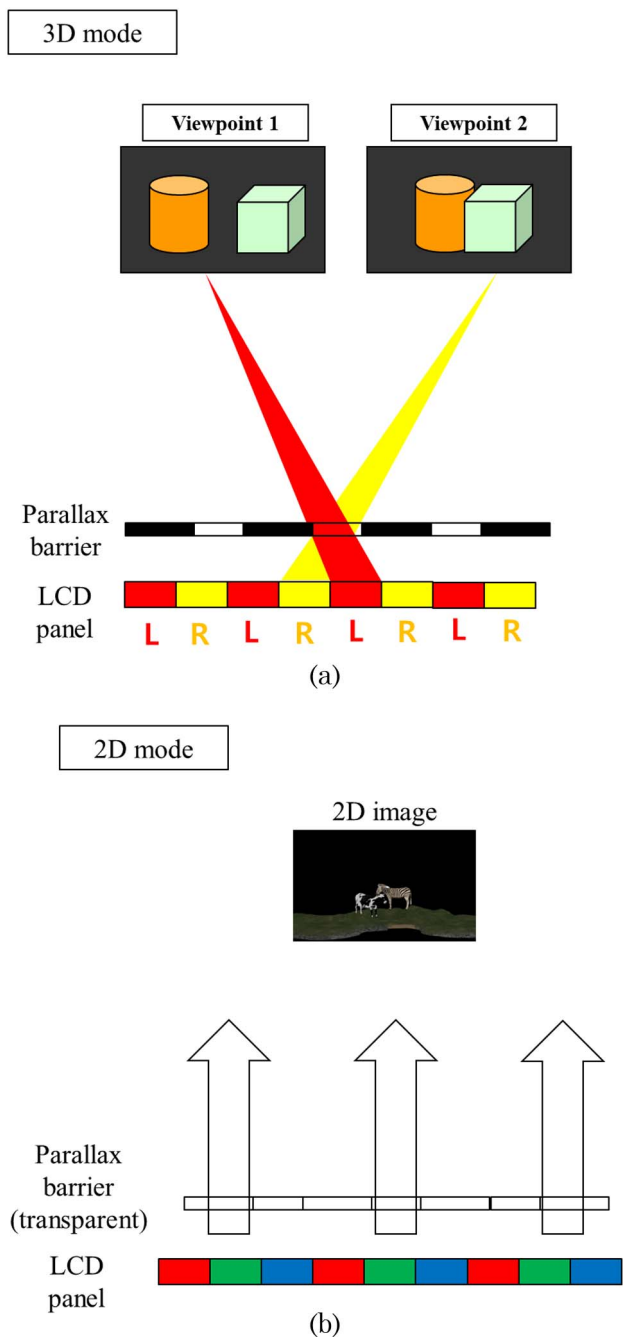(transparent)

LCD
panel

(b)

Fig. 8. (Color online) Operation of a 2D/3D convertible parallax barrier display using an LC panel: (a) 3D mode and (b) 2D mode.

lens display because it also uses pixel multiplexing to impose left and right images. A more severe problem is a reduction of the brightness of images because it blocks light from pixels with masks to implement an autostereoscopic feature. It becomes worse for a multiview case because the total area of the mask is increased. Despite those disadvantages, parallax barriers are popular autostereoscopic technology among manufacturers because they can be easily implemented without an additional optic element and provide a 2D/3D convertible feature by using an LC panel as a vertical mask. By simply displaying

an image of an array of vertical masks on an additional LC panel, a 3D display mode is utilized. A 2D display mode can be achieved by displaying a white image on an additional LC panel. The LC panel becomes just a transparent glass and the 2D image on the display panel behind is directly shown to the observer, as shown in Fig. 8(b). Another advantage of adopting an LC panel as an array of vertical masks is that it can be used to resolve a reduction of resolution. Basically, a reduction of resolution comes from the situation where the information of an image is given only through the location of each slit. By continuously shifting an array of vertical masks with a step size of slit pitch, the full resolution of the display panel can be perceived by an observer. Although it requires a higher frame rate for display panels incorporated in a system to provide a natural afterimage without flickering, a series of investigations are being conducted to resolve the reduction of resolution by using this scheme [13,14].

Sharp has already tried to distribute commercial cell phones adopting a parallax barrier through the vendor NTT DoCoMo in Japan, in 2002. However, the result was not successful because of a lack of compatible contents. A second trial was made by Samsung Electronics in Korea in 2007. A cell phone with a parallax barrier feature was released by Samsung Electronics and it even had a stereo camera to overcome a lack of contents. However, the 3D display feature was not emphasized at all for marketing and it left no impressive mark in the history of 3D display. On June 2011, LG Electronics globally released a smart phone with a parallax barrier and stereo camera and the 3D display feature is a main marketing point for this product. Many people believe that this third trial of a commercial autostereoscopic product will be successful because of the positive mood in the 3D display industry and an increasing amount of compatible contents.

C. Integral Imaging

Integral imaging, originally called integral photography, is a promising 3D display technique with more than 100 years of history [15]. It was the first proposal among autostereoscopic displays, such as the lenticular lens method, the parallax barrier method, integral imaging, and even holography. Integral imaging uses an array of small lenses that are spherical, square, or hexagonal to produce the 3D images, which can provide both a horizontal and a vertical parallax, resulting from a 2D lens array. Unfortunately, the reason that integral imaging did not prosper in the early days was that lens arrays were not economically feasible for practical use until World War II. Before then, a pinhole array, which is optically equivalent to the lens array, had been used for most integral imaging research. However, the 3D image with low brightness, which results from the small pinhole aperture size, was not proper for a commercial use. Another reason that integral imaging was not attractive in the early years of invention

was a recording device. The first integral imaging was "integral photography," which was to record a complete spatial image on a photographic plate with a horizontal parallax as well as a vertical parallax. The method was a huge breakthrough for 3D display; however, the methods of using photographic plates for recording and displaying an image were not suitable for moving objects. The bottleneck was overcome by mass production of microlens arrays and the development of active recording and displaying devices, such as high-resolution digital cameras and 2D FPD devices. Hence, the technologies enabled integral imaging to evolve as a real-time process system [16].

The structure and concept of the integral imaging system are illustrated in Fig. 9. In the pickup step, each individual lens or pinhole will record its own microimage of the object, which is called the elemental image, and a large number of small and juxtaposed elemental images will be produced behind the lens array onto the recording device. In the display step, the display device with the elemental image is aligned with the lens array and a spatial reconstruction of the object is created in front of the lens array, which can be observed with arbitrary perspective within a limited viewing angle. Therefore, integral imaging suffers from inherent drawbacks in terms of viewing parameters, such as viewing angle, resolution, and depth range, due to the limited resolution of the 2D FPD and lens array itself [17].

In spite of much recent advanced research on integral imaging, most can be categorized into two methods: a real/virtual display mode and a focused display mode [18–20]. The difference between the modes, as shown in Fig. 10, is the gap between the 2D lens array and the elemental image on the display device. In the focused display mode, the gap between the 2D lens array and the elemental image is equal to the focal length of the lens array. This was the original integral photography proposed in 1908 [15]. In this mode, the rays from each elemental image pixel are collimated by the corresponding elemental lens in the ideal case, so the resolution of the recreated 3D image is deteriorated, resulting from magnification of the elemental lens. As regards the depth

range of the focused display mode, in theory, it provides a wide range of depth because the beam waist from each ray bundle is minimized at the lens array and it increases as the beam propagates. In this focused display mode, both real and virtual images can be integrated with about the same resolution. In contrast, in the real/virtual display mode, the gap is set to be larger or smaller than the focal length of the lens array. Therefore, the image distance with good focus of the image of each ray bundle from the elemental image pixel is determined by the focal length of the lens array and the gap between the 2D lens array and the display device in accordance with the Gauss lens law. The recreated 3D image is formed around the image plane of the 2D lens array. Here the image plane is called the central depth plane (CDP). As the reconstructed point of the 3D image goes away from the CDP, the beam waist from each ray bundle increases, which results in degradation of the recreated 3D image. In other words, the real/virtual display mode is better in image quality of the reconstructed 3D image around the CDP and the depth range of the 3D image is limited around the CDP.

The limitation of viewing angle occurs when the elemental images are observed not through corresponding elemental lenses but through neighboring lenses. Each elemental lens has its corresponding area in the elemental image plane, and the elemental images should be placed inside the corresponding area in order to prevent cracking or flipping of the reconstructed 3D image. The viewing angle is determined by the pitch of the lens array and the gap between the lens array and the display device. The individual ray bundle from an elemental image pixel can be distributed by the lens array, so the number of perspectives within the viewing angle is understood as angular resolution. If other conditions, such as the pitch of the elemental lens and the gap between the lens array and the display device are equal as the resolution of display device increases, then integral imaging can provide more natural views because of high angular resolution density [21]. A super-multiview condition can be achieved when the angular resolution density of an individual ray bundle is high enough to provide a number of views into the single eye [22].

The distinctive feature of integral imaging compared to the lenticular lens method or parallax barrier method is to use a 2D lens array. The 2D lens array structure enables both horizontal parallax and vertical parallax to be provided. However, the main trade-off for the full parallax is lower resolution of the reconstructed 3D image compared with previously mentioned autostereoscopic display techniques, such as the lenticular lens method or the parallax barrier method. This is the main reason that researchers in industry prefer a one-way parallax, mostly the horizontal-parallax-only (HPO) method, rather than integral imaging. However, as the resolution of 2D FPDs increases, the resolution
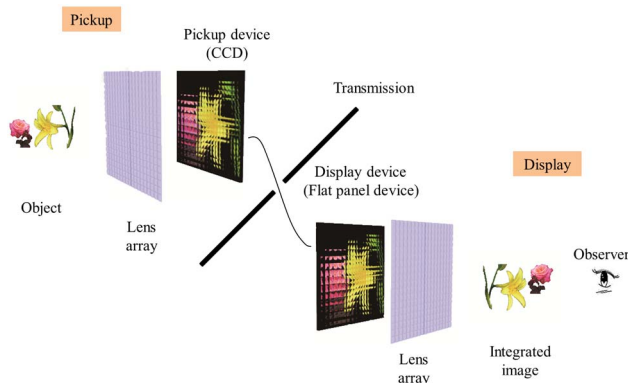

Fig. 9.   (Color online) Structure and concept of integral imaging.
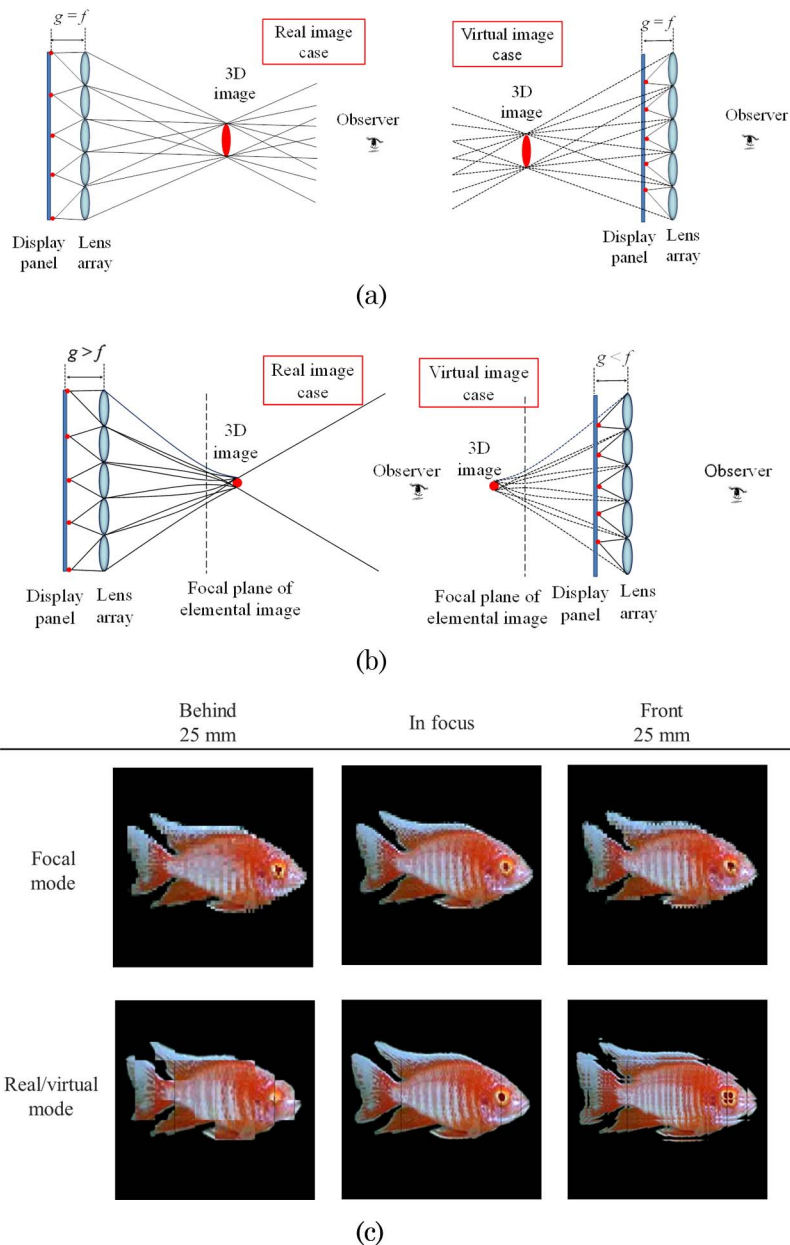
(a)

(b)

(c)

Fig. 10. (Color online) Display modes of integral imaging: (a) focal display mode, (b) real/virtual display mode, and (c) simulation results of reconstructed 3D image in focal display mode and real/virtual display mode. For the simulation of focal display mode, a 1 mm × 1 mm lens array with focal length of 3 mm was assumed. For the real/virtual mode, a 10 mm × 10 mm lens array with focal length of 30 mm was assumed and the CDP is located 90 mm in front of the lens array. The pixel pitch of the display is 0.08 mm × 0.08 mm for both cases. In this figure, distortion of the reconstructed image at two locations out from the in-focus plane is compared. In ISP data, a change in the distortion level of the reconstructed image can be explored according to its location from the in-focus plane (View 1).

of 3D images based on integral imaging is expected to be higher in the near future. Therefore, integral imaging can be an alternative, lying between stereoscopic display and holography. Another issue with regard to 2D lens arrays is the color moiré pattern, which can degrade the image quality of integral imaging [23,24]. The color moiré pattern usually comes from the periodicity of overlapped similar structures of color pixels and the 2D lens array. Typically, the 2D flat panel device that provides elemental images expresses arbitrary color images by the combination of red (R), green (G), and blue (B)

pixels. Although each pixel has an individual arrangement and different size, they have periodicity. Because of similar periodicity of the 2D lens array, the former interferes with the periodicity of the 2D lens array. In such a case, a visible color periodic pattern (usually vertical lines) will be generated (In general, projection-type integral imaging is free from the color moiré pattern problem.) [25]. To resolve the moiré pattern in integral imaging, some methods have been proposed as alternatives. The simplest method is to break the periodicity of overlapped structures—a color pixel array or a lens array. The

former can be implemented by changing the layout of the color filter on the FPD device [23], and the latter can be effective when a slanted lens array is placed in juxtaposition with display device [24]. Because a change of the layout of the color filter is hampered by a variety of restrictions, the slanted lens array method is a viable alternative for the color moiré pattern problem. Figure 11 shows the simulation results according to the rotated angle of the lens array on the display panel.

Since the viewing parameters discussed above have a trade-off relationship, the simultaneous enhancement of them is possible by manipulating each component of integral imaging. Some theoretical studies on these issues that use ray optic analysis as well as wave optic analysis have been reported [18,26,27]. Theoretical analysis for integral imaging performance was also quantitatively done [28]. In the following, we shall focus on reviewing recent research to mitigate those issues. Display hardware systems for enhancement of viewing parameters in integral imaging will be presented.

One of the challenging problems in integral imaging is extending the viewing angle. Once the pitch of the elemental lens and the gap between the lens array and the display device are set, the viewing angle is also determined. The viewing angle enhancement can be accomplished by enlarging the area in the elemental image that corresponds to each elemental lens or altering the structure of the lens array. One of the best ways to deploy the elemental image area is using mechanical dynamic movement of the lens array or barrier [29–32]. Moving the lens array in synchrony with a high-speed update of the pixel content can increase the viewing angle
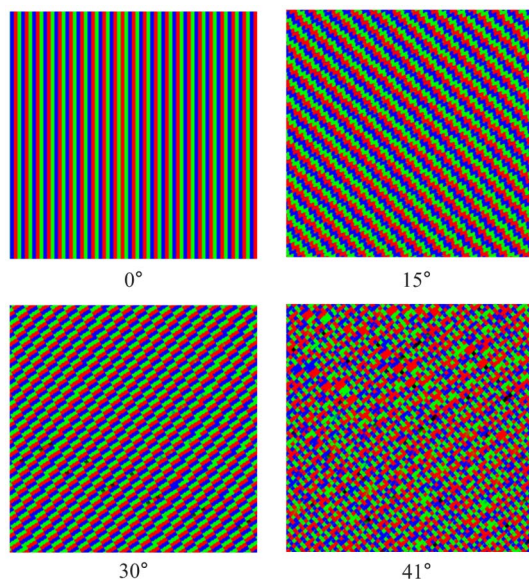
[29]. Another approach for enhancing the viewing angle without mechanical movement of optical components is to double the region of each elemental image by using orthogonal polarization switching [33]. Another recent approach to improve the viewing angle of integral imaging is to apply an adaptive elemental image by using a head tracking system, which is effective only for a small number of users [34], as shown in Fig. 12(a). The methods to modify the configuration of the lens array or display device are notable [35–40]. A horizontal viewing angle of 66° for 3D images was achieved experimentally using a curved lens array and screen, as shown in Fig. 12(b) [37], and a 360° viewable integral imaging system using flexible backlight was implemented [38]. Instead of changing the total structure of the lens array or screen, an embossed screen for projection-type integral imaging was proposed [39]. The use of a multiple axis telecentric relay system, which allows the substantial increase of the field of view (FOV) of any microlens, provides the elemental images with proper directions, increasing the viewing angle of integral imaging [41]. A theoretically investigation was reported by using a negative refractive index planoconcave lens array and inserting a high-refractive-index medium between the elemental image and the lens array [42,43]. In addition, enhancing the uniformity of the angular resolution within the viewing angle by using boundary folding mirrors was recently studied [21].

Resolution enhancement is mainly achieved by increasing the bandwidth of the information on the display device, which can be done by reducing the

Fig. 11. (Color online) Simulation results according to the rotated angle of the lens array on the display device. For the simulation, a 1 mm × 1 mm lens array with focal length of 3 mm is assumed. The pixel pitch of the display was 0.1 mm × 0.1 mm and the rotation was counterclockwise (View 2).
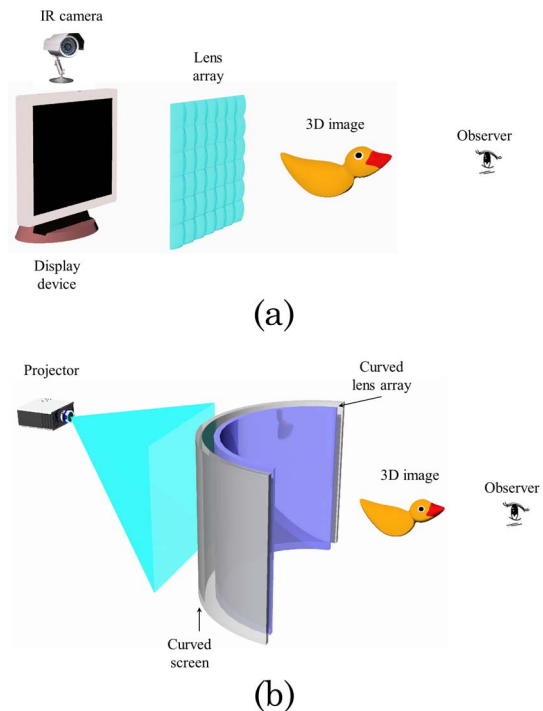

Fig. 12. (Color online) Examples of a viewing angle enhancing configuration: (a) tracking method; (b) curved lens array.

pixel size of the display device and using a temporal or spatial multiplexing scheme [44–47]. Recently, with the rise of the development of 2D FPD devices, an HD display device has been used for providing enhanced 3D image resolution. However, an electrically or mechanically moving lens array (pinhole array) method or rotating prism sheet method can be an alternative for better viewing resolution because there is a physical limit to the reduction of the pixel size of a display device [28,29,44,45]. The spatial multiplexing method is mainly performed by tiling display devices for the entire elemental image, as shown in Fig. 13 [46,47]. In this case, alignment between the elemental images and the lens array arrangement is another important issue.

Although integral imaging can provide depth range to some extent, the simplest way to achieve depth range enhancement is to create multiple image planes (or CDPs) of elemental images by combining plural display devices because the depth range is formed around the CDP. Figure 14 shows some examples of the configuration for enhancing image depth range. Depth range enhancement can be realized by mechanically moving the elemental image plane, stacking display devices, such as an LCD or polymer dispersed liquid crystal (PDLC), and using a birefringent plate [48–55]. Another approach for depth range enhancement is to combine floating displays with integral imaging [56–62]. By using a large convex lens or a concave mirror to display the image of an object to the observer, the floating display method can provide an impressive feel of depth. Although the image source of an integral floating display is provided by the integral imaging method, the reconstructed image produced by an integral floating display has different viewing characteristics compared with the reconstructed 3D image achieved by the integral imaging method.

2D/3D convertible display is an important issue for the penetration of the 3D display market because it can be a stepping stone between 2D and 3D display. In integral imaging, various types of 2D/3D convertible display have been proposed, as well. The key
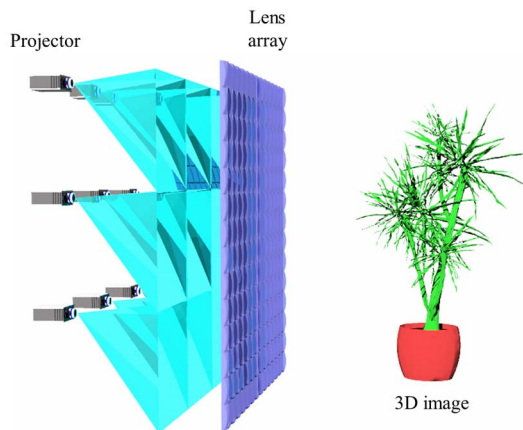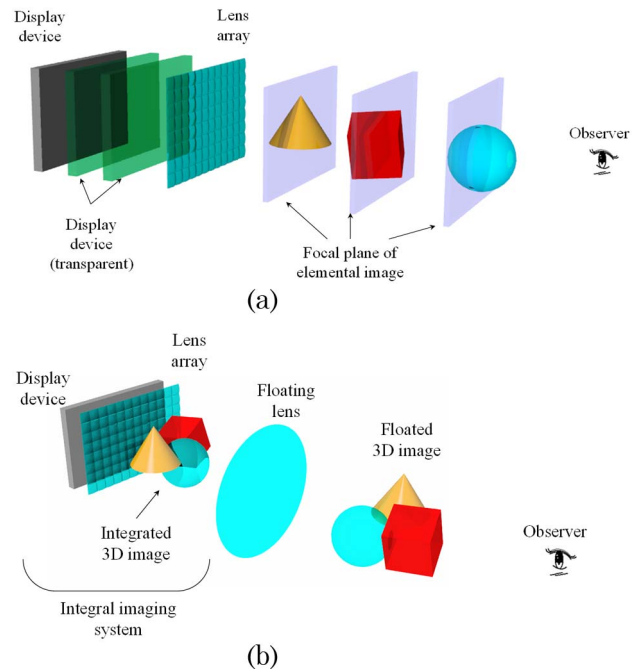

Fig. 14. (Color online) Examples of a depth range enhancing configuration: (a) multiple focal planes of elemental images; (b) integral floating display.

issue of the 2D/3D convertible integral imaging method is controlling activation of the lens array or pinhole array. In one approach, the activation can be achieved by an electrically controllable diffuser made of PDLC or transparent LCD panels [63,64]. Finally, for controlling a point light source array, various methods have been reported that use pinholes on a polarizer, a light-emitting diode array, a plastic optical fiber array, an OLED panel, or a punctuated electroluminescent film [65–70].

Recent progress in autostereoscopic displays is focused on the enhancement of 3D resolution, as well as smooth parallax. Although integral imaging provides both vertical and horizontal parallax within a limited viewing angle, low resolution resulting from full parallax is still a problem for practical use. Recently, a 21 in. 3D LCD TV with high definition (1280 × 800) was revealed, which is one of the best commercial integral imaging systems using 2D FPD. However, it is not practical yet because of the need for a UHD panel, the manipulation of the microlens array, and an alignment issue between the lens array and the display device. For example, for achieving resolution of 200 × 200 and a ray density per single elemental lens of 5 × 5, we need an extended graphics array (XGA) panel (1024 × 768) at the least. When it expands to the smooth parallax for natural views, a UHD panel will be necessary for the same 3D resolution of the reconstructed image. Currently available FPDs, on the contrary, provide full-HD resolution (1920 × 1080) and a 120 or 240 Hz refresh rate. The resolution of the 3D image is expected to be the resolution of full HD or its equivalent. However, the resolution remains that of

Fig. 13. (Color online) Spatial multiplexing configuration of projectors for enhancing the resolution.

XGA resolution in practice, even though a UHD panel and a fine microlens array are used. Therefore, to process the high-density information of integral imaging in real time, for a display device that has higher resolution than a UHD device, fast LC response time with a high-speed driving circuit and microlens manufacturing technology are necessary for mass production. As in the lenticular lens system, electrically controllable 2D LC lens arrays represent a good research direction.

5. Holography

Holography was invented by Gabor as a then-new concept of electron microscopy [71]. This technique presents feasibility in reconstructing signal waves with magnification. Holography then received lots of attention after the development of laser technology. Leith and Upatnieks proposed off-axis holography to separate a signal from its autocorrelation and conjugate with the carrier frequency [72]. Various media for recording were applied and developed over the same period. The volume hologram was invented by Denisyuk and it records interference on a thick reflection hologram [73]. This invention was regarded as work originating from a color photography plate introduced by Lippmann [74].

The first digital hologram was computed and implemented by Lohmann and Paris [75] and the principle of digital holography was expanded on by Goodman and Lawrence [76]. Digital holography technology has powerful potential to record an optical wave and reconstruct it dynamically using electro-optical devices. Originally, digital holography meant reconstruction of a hologram by using a computer. Currently, however, this terminology is widely used for representing holography using electronic devices or computers in either recording or reconstruction. Even though there have been notable improvements in recording techniques [77–79], it is regarded as impractical to capture the interference between a reference wave and a signal wave reflected from real dynamic objects. As computational power increases, computer-generated holography is expected to be a promising technology to provide contents for digital holographic display.

A. Principle

Digital holography is realized with electro-optical devices for recording and reconstruction. Since most electro-optical devices have rectangular sampling lattices, the signal measured or retrieved by them fundamentally follows the Whittaker–Shannon sampling theorem. Even though any band-limited function cannot be perfectly space limited, it is possible to represent a band-limited function with a finite number of samples with practical accuracy. The product of the area of the sampled space and its bandwidth is referred to as the space–bandwidth product (SBP). When the optical signal is reconstructed by the digital holographic method, the SBP of this wave has a finite number and its value is equal to the number of sampling points in the electro-optical device retrieving the wave [80]. That is, if the number of sampling points is fixed in an optical system, the SBP is also determined as the same number. For example, a spatial light modulators (SLM) has a finite number of pixels and this number represents its SBP. For a given SLM, it is impossible to increase the size of the reconstruction image without the cost of its bandwidth.

In holography, an SLM is mostly applied as an amplitude-only or phase-only modulation device for reconstructing a desired wave, even though the technique for realizing complex modulations has been studied and implemented. As Oppenheim and Lim pointed out [81], the phase in a signal has more important meaning than its amplitude information, especially in Fourier transform. In practice, there is a benefit to designing a display system with Fourier transform since the autocorrelation of the collimated reference is focused on a point and it may be easily filtered out. In Fourier transform, a view volume reconstructed by an SLM is bounded as a wedge shape, as shown in Fig. 15, when we consider the overlap among higher-order diffraction terms [82]. The signal bandwidth free of aliasing is identified as the Nyquist frequency and its replica array is arranged in a rectangular lattice. Hence, higher-order terms determine a view volume in 3D space and, inside it, a diffracted wave is displayed without conflicts by its replica.

The displayed view volume has transverse and longitudinal resolutions since the SBP is finite. The resolution of the view volume is determined by the Fourier uncertainty relationship, meaning that the resolution is inversely proportional to the bandwidth [83]. Since the angular spectrum is a Fourier transform of the signal, the bandwidth at the SBP can be understood as the bandwidth of the angular spectrum. Therefore, the resolutions are given by $\lambda z_0/A$ in the transverse coordinates and $8\lambda z_0^2/A^2$ in the longitudinal coordinate, where λ is the wavelength used for a digital holographic display system and z_0 is the distance from the Fourier transform lens to the position of interest in a view volume. The aperture size A is regarded as the width of the SLM that is equal to the width of the sampled area.

In a similar sense, the quality of the reconstructed wave is delicately evaluated as a quality metric [84]. In general, we assume that a point is reconstructed by an SLM without an additional optic device or lens. In this case, if a propagation distance is very small, the bandwidth of a reconstruction point is equal to the maximum bandwidth of the SLM, but only a small portion of it contributes to reconstruction in consideration of the Nyquist frequency. On the other hand, if a propagation distance becomes large enough, its bandwidth decreases in inverse proportion to the distance. Therefore, a quality metric increases within some distance and then it decreases. The distance to get a maximum quality metric is determined

$$\frac{\lambda f^2}{Np^2 + (f-d)\lambda}$$

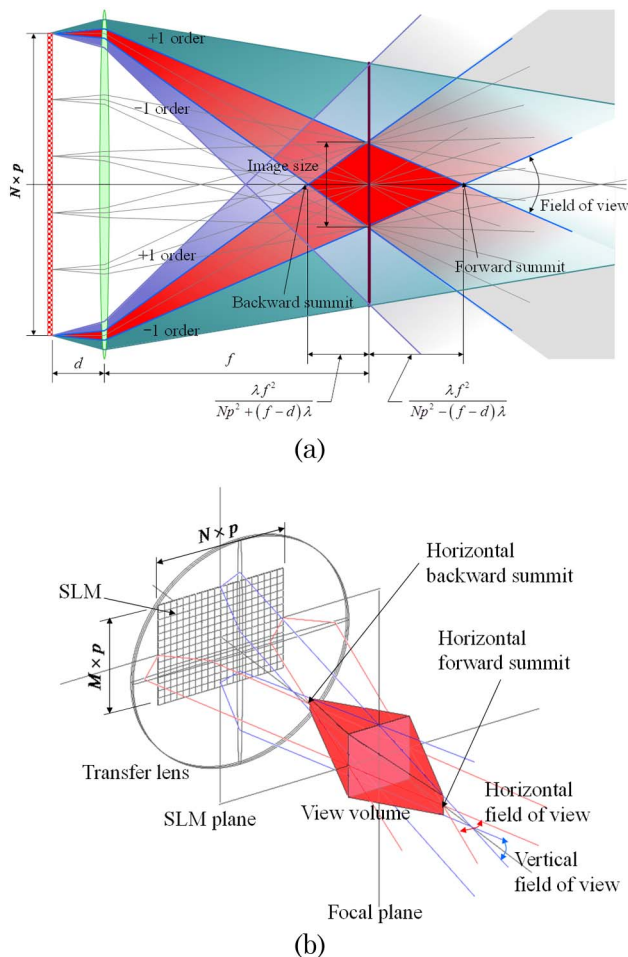$$\frac{\lambda f^2}{Np^2 - (f-d)\lambda}$$

(a)

(b)

Fig. 15. (Color online) View volume displayed by a single SLM. (a) View volume is determined by overlap among higher-order diffraction terms. (b) It has a wedge shape and its angle represents the field of view.

by the sampling interval and the total size of the SLM.

B. Issues

Even though digital holographic display is regarded as an ideal 3D display, there still remain several issues to overcome. In this paper, we discuss some of the noteworthy issues and introduce recent studies to solve these problems.

In digital holographic display, the 3D view is reconstructed following the SBP, and the size of the image and the FOV are related to one another; their product is equal to the number of samples in electro-optical modulators [85]. Since the optical wavelength in the visible range is so small in comparison with the size resolvable by the human eye, a huge number of pixels in the SLM is necessary to reconstruct digital holographic view volume with reasonable dimensions. For example, to reconstruct a 350 mm × 350 mm image size holographic display with full parallax of FOV of 20°, we need about 60 gigapixels in the SLM. This number is too huge for implementation. Hence, in digital holographic display, a technique to reduce

the required number of pixels in the SLM is one of the most important issues. Many studies have applied asymmetric optics to abandon vertical parallax and these approaches succeeded in decreasing the required SBP significantly. Therefore, HPO holography is regarded as a practical solution in current technology.

The image reconstructed from a hologram generally has a "speckle" phenomenon, which appears as a high-contrast, fine-scale granular pattern. This phenomenon originates from interference of coherent light reflected from rough surfaces [86]. Since digital holography is based on the coherence of light, it is intrinsically inevitable. In speckle, the contrast naturally depends on the amount of coherence of light, and the fineness of the granular pattern depends on the numerical aperture of a system. Therefore, to lessen this speckle phenomenon, researchers have tried to decrease the coherence of light and multiplex several images with speckle to obtain the averaged intensity of them.

The ghost is also considered an undesirable phenomenon in digital holography. Originally, this word meant the convolution image between a small fragment of the object field and the whole object field [87]. Even though only one part of the object field is used to reconstruct the hologram, the whole object field appears resulting from their convolution. Currently, however, this is frequently used to mean a noise that looks hazy in the reconstruction image and sometimes it is used to describe autocorrelation or the twin conjugate of a signal. This is expected to be solved by enhancing the quality of light sources, optics, and their alignments.

Another practical problem in digital holography is recording dynamic objects. In real applications, it is not easy to record real object fields by a focal plane array (FPA) since the visibility of interference abruptly falls when the movement of an object is considerable in comparison to the optical wavelength and exposure time of the FPA. Since there exists a limitation in reducing the exposure time, it is regarded as a more reasonable approach to use a pulse laser for recording in a short time [88]. In addition, the turbulence of the air through which the object wave passes also arises as a problem for recording and there have been many studies to correct this kind of aberration by an optimization algorithm [89]. In parallel, the methods to generate a hologram by computer have been deeply studied and the computation time has been remarkably reduced. Hence, if the contents for digital holography are generated computationally, it is expected that there will be no significant obstruction to achieve it.

C. Status

Digital holographic display has been studied by many research groups and it is meaningful to introduce some remarkable systems. Stanley *et al.* presented a 100 megapixel holographic display and they have a record as a system with the largest

number of pixels [90]. This system is composed of four channels, where each channel has one electrically addressed (EA) SLM and correspondent optically addressed (OA) SLMs. One EA SLM has 1 megapixel and distributes its information to 25 OA SLMs sequentially. Hence, one channel reconstructs an optical field with 25 megapixels and eventually the whole system has 100 megapixels. This system is designed to display images with 140 mm × 70 mm size and its horizontal FOV is 5.3°.

Another possible approach is to form a view window [91]. Instead of trying to enlarge the viewing angle that accompanies a reduction of the 3D image size or an increase of the SLM bandwidth requirement, the view-window method generates small windows around the observer's eyes. The 3D image is displayed such that it can be observed only through the window. Since each point of the 3D image is reconstructed only within a narrow angular range, the SLM bandwidth requirement is much reduced. Although the narrow angular range results in some loss in the resolution of the displayed 3D image due to reduced effective numerical aperture (NA), the loss is not perceived by the observer since the reduced NA is still larger than that of the observer's eye. One drawback of this method is that the observer's position is fixed where the view window is generated. Hence, viewer tracking technology with an optical system to steer the location of the view window is additionally required to enlarge the effective viewing angle.

Figure 16 shows the principle of view-window generation. With an SLM of around a few tens of micrometers pixel pitch that is currently available, the maximum diffraction angle is given under 1° or 2°. When a collimated laser illuminates the SLM in the normal direction, each point on the SLM diffracts the incident light within this angular range in the normal direction, as shown in Fig. 16(a). By illuminating the SLM with a converging laser beam, the diffracted light converges, generating a view window, as shown in Fig. 16(b). The view-window size is given approximately by $2\theta d = d\lambda/p$, where θ is the diffraction angle, d is the view-window distance or focal length of the lens for converging illumination, λ is the wavelength, and p is the pixel pitch of the SLM. For $d = 750$ mm, $\lambda = 532$ nm, and $p = 30\,\mu$m, the view-window size is 13.3 mm, which can cover a single eye of the observer. When the observer locates his/her eye within this view window, a large size 3D image can be seen on the whole SLM area. Therefore, in essence, the view-window method enlarges the 3D image size at the sacrifice of viewing angle for a given SLM bandwidth. Again the limitation in the viewing angle can be relieved by a viewer tracking system.

In a usual hologram, the elementary hologram for each 3D image point covers the whole area of the SLM. In the view-window method, however, the elementary hologram for each image point has a limited SLM area due to the narrow angular reconstruction range. This type of hologram is called a subhologram.
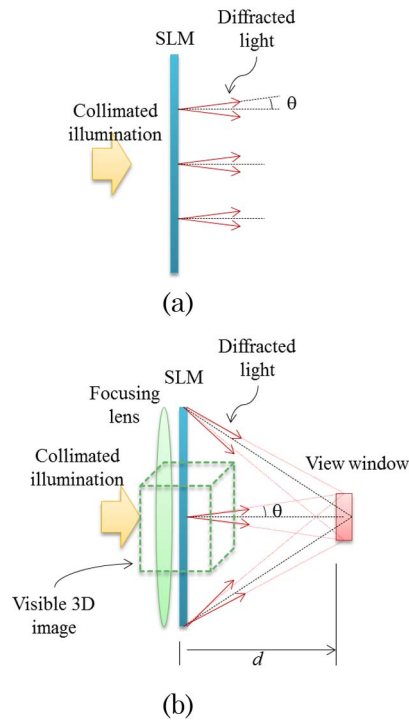

Fig. 16. (Color online) View-window formation in a holographic 3D display. (a) Diffracted light does not converge. (b) Diffracted light converges to form a view-window.

Figure 17 shows the concept of subholograms. Unlike the usual hologram shown in Fig. 17(a), the range of a subhologram is limited to the area corresponding to the view window, as shown in Fig. 17(b). This reduced area contributes to the reduction of the computational load. In summary, the view-window method has an advantage that a large size 3D image can be displayed with a currently available SLM. The
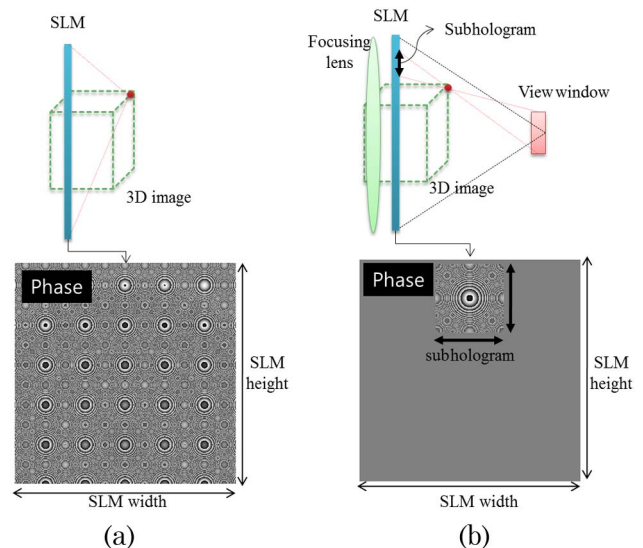

Fig. 17. (Color online) Concept of a subhologram. (a) Usual hologram where the whole SLM area contributes to reconstruction of each 3D image point. (b) Subhologram where only the area corresponding to the view window contributes to the reconstruction.

requirement of the view-window steering system, which is not easy to implement, however, is a drawback.

An interesting display system that uses time multiplexing was proposed by Takaki's group [92]. It is implemented by a digital micromirror device (DMD). Since the DMD is a binary amplitude modulator, the undiffracted term originated from autocorrelation of a reference and the twin conjugate of a signal are optically filtered out. The aspect ratio of the reconstructed image is determined by anamorphic imaging optics and the imaging position is determined by a mechanical scanner. Since the DMD used as an SLM represents only binary information, reconstructed images are designed to be overlapped with each other to improve the quality of the time-averaged view. Furthermore, this average is claimed helpful to reduce annoying speckle phenomenon.

D. Holography Synthesis Using Integral Imaging

Hologram recording of real objects has been studied for a few decades. By illuminating the object with a coherent light and interfering the object wave with a reference wave, the hologram of the object can be recorded. After the advent of the digital holography that uses a CCD as a recording medium, instead of holographic film, it also became possible to extract the complex field of the object and apply digital processing [93]. This traditional method, however, requires a well-controlled laboratory environment for recording minute interference patterns. Hence, it is not possible to capture a hologram of a general 3D scene outside of the laboratory. This fact is an especially severe limitation in the aspect of content generation for holographic 3D displays.

Recently, active research has been conducted to relieve this limitation. One approach is to synthesize a hologram of the 3D scene from multiple perspective images captured under usual incoherent white illumination [94]. For a given 3D scene, a number of different perspectives are captured by either a camera array or a moving camera system. The captured perspectives are processed, considering corresponding ray directions with suitable phase factors to synthesize the hologram of the scene. Another approach is to use integral imaging [95,96]. Instead of capturing multiple perspectives using a complicated system, this method captures a set of elemental images of the 3D scene using a lens array under the integral imaging principle. The captured elemental images are processed to create a number of different subimages of the 3D scene. Note that the subimage has an orthographic projection geometry where the projection lines are parallel. Considering this parallel projection geometry, the created subimages are processed to synthesize the hologram of the captured 3D scene. The single capture process and parallel projection lines of integral imaging make the hologram synthesis process more efficient and precise. Figures 18(a) and 18(b) show an example of the captured elemental images and the subimages created from them. The hologram is synthesized using the created subimages, as shown in Fig. 18(c). Figure 18(d) shows numerical reconstruction results of the synthesized hologram at various distances. It can be observed that each object of a 3D scene is focused at a different distance, which confirms the 3D nature of the synthesized hologram. These methods of using multiple perspectives or integral imaging allow capturing a hologram of a real 3D scene in an outdoor environment like usual 2D content capture, which makes it feasible to generate contents for holographic 3D displays. However, the holograms
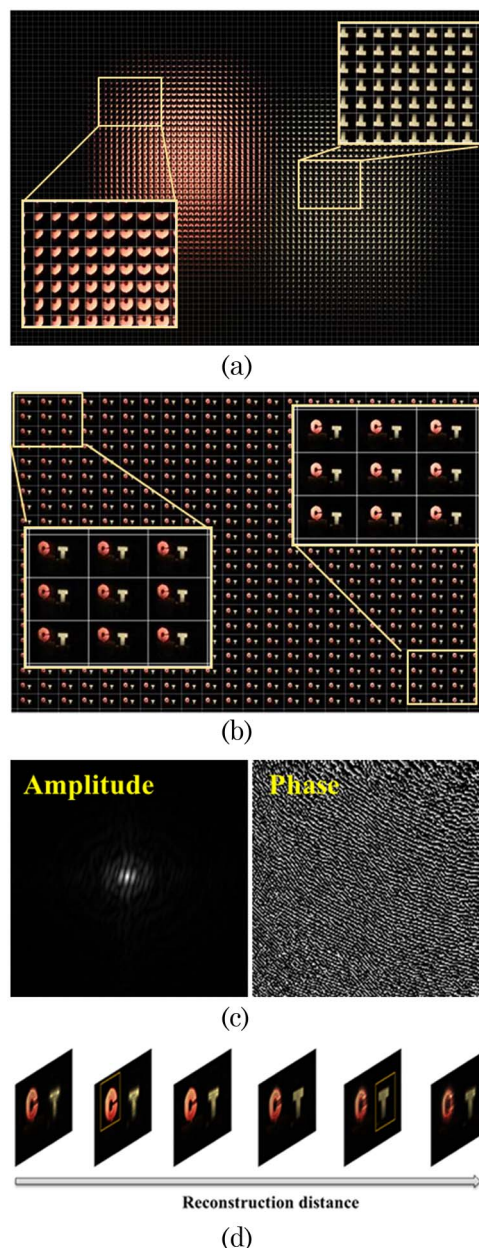

(a)

(b)

(c)

(d)

Fig. 18. (Color online) Hologram synthesis using integral imaging: (a) capture set of elemental images, (b) subimages generated from elemental images, (c) synthesized hologram, and (d) numerical reconstruction at various distances (View 3).
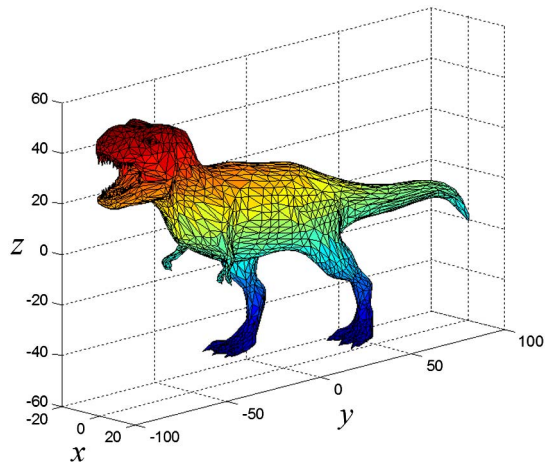
Fig. 19.   (Color online) Triangular-mesh object.

synthesized by these methods have generally lower resolution than traditional holograms that are based on coherent interferometers, reserving large room for further enhancement.

E.   Triangular-Mesh-Based Computer-Generated Hologram

A synthesis algorithm of a computer-generated hologram (CGH) based on a triangular-mesh model has been introduced [97]. Standard software for 3D computer graphics produces triangulated mesh data for describing arbitrary 3D curved objects. An example of a triangular-mesh object is shown in Fig. 19. A 3D volumetric object is basically composed of a closed set of triangles. In practice, for an observer at a specific observation position, part of the triangles in the full set of triangles of a 3D object can be observed. According to this occlusion effect, the set of triangles can be divided into two distinct sets of triangles: visible triangles and invisible triangles. This algorithmic problem is called the visibility problem of a 3D object.

An efficient solution of the visibility problem is provided by graphics card hardware. We can exploit the efficient and fast classification ability of graphics card hardware. In Figs. 20(a) and 20(b), the front view of a 3D object and the partial set of visible triangles corresponding to the front view of the 3D
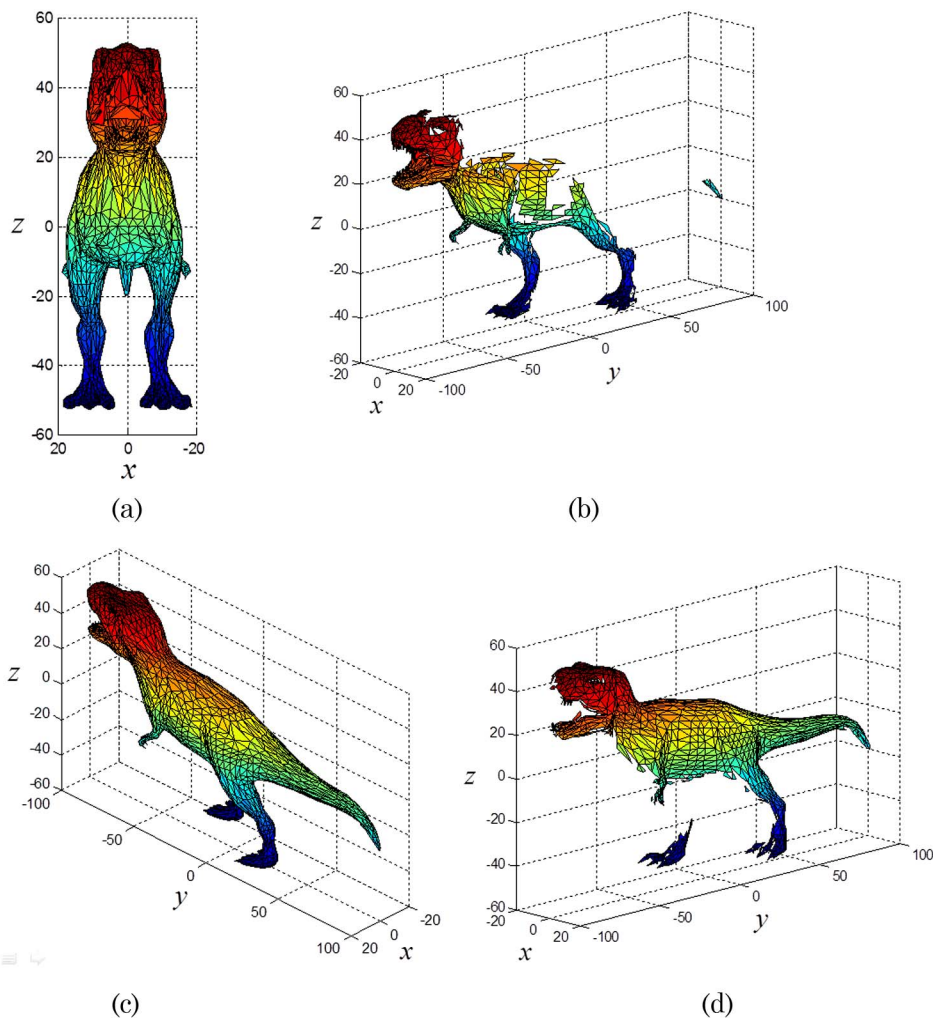

(a)

(b)

(c)

(d)

Fig. 20.   (Color online) Visibility problem: (a) front view of a 3D object and (b) the corresponding set of visible triangles; (c) perspective view of a 3D object and (d) the corresponding set of visible triangles.

object are presented, respectively. Invisible triangles are not drawn in Fig. 20(b). In Figs. 20(c) and 20(d), a different perspective view of the same 3D object and the corresponding set of visible triangles are presented. A graphics card supports almost real-time processing for separating visible and invisible triangle groups.

The basic unit of CGH is the angular spectrum representation of a tilted triangle with arbitrary direction. After grouping the visible triangles of a 3D object for a specific observation position, the angular spectrum representation of all visible triangles with their own tilt directions are computed and summed up coherently to produce a complex 3D image light field. The mathematical model of the angular spectrum representation of a tilted triangle was developed in [97]. In Fig. 21, a part of the triangular-mesh surface with a diffusive surface that is represented by subdivided triangulation is shown. For a tilted triangle facet, the angular spectrum representation is first formulated in the local coordinate of the facet denoted by (x', y', z'), and then the angular spectrum is reformulated in the global coordinate system (x, y, z) by a rotational transformation. The diffusiveness or texture effect of a triangle facet can be realized by phase and amplitude encoding on subdivision triangles of a triangle facet.

In Figs. 22(a) and 22(b), a CGH synthesis setup and display setup are illustrated, respectively. In the configuration of optical Fourier transform, the light field radiated from the surface of the 3D object is numerically recorded through a Fourier transform lens with a focal length of f. As a result, the CGH is equivalent to angular spectrum representation of the visible surface of the 3D object. The recorded angular spectrum CGH can be replayed by the same Fourier transform system, but the x axis and y axis must be inverted in the case of CGH display, as shown in Fig. 22(b).

The recorded CGH is 2D complex field distribution. Ideally, the complex modulator is necessary for modulation of both the amplitude and phase profiles of an incident beam. The complex modulator is

Fig. 22. (Color online) (a) CGH synthesis setup and (b) CGH display setup.

particularly required for 3D holographic displays. Observation simulation results of the holographic 3D image of the 3D model shown in Fig. 19 are presented in Fig. 23. Observers see the 3D holographic image at different depth planes. It is shown that the
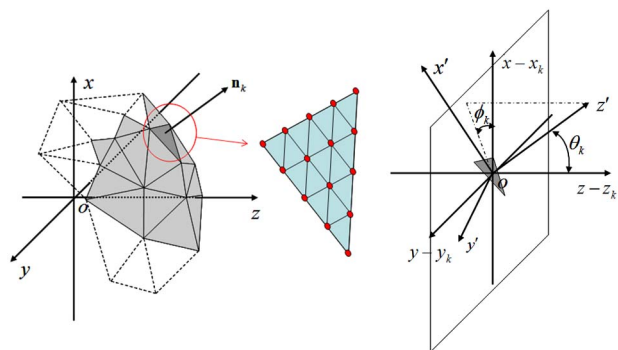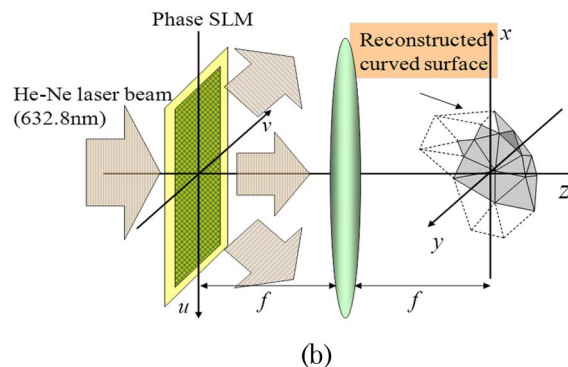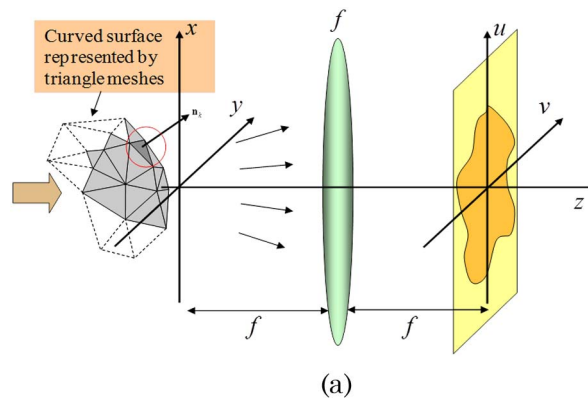

Fig. 21. (Color online) Angular spectrum representation of arbitrarily tilted triangle aperture. A triangle facet is subdivided into several identical triangles on the same plane. A texture effect on a triangle facet can be realized by encoding complex numbers on each subdivision triangle.
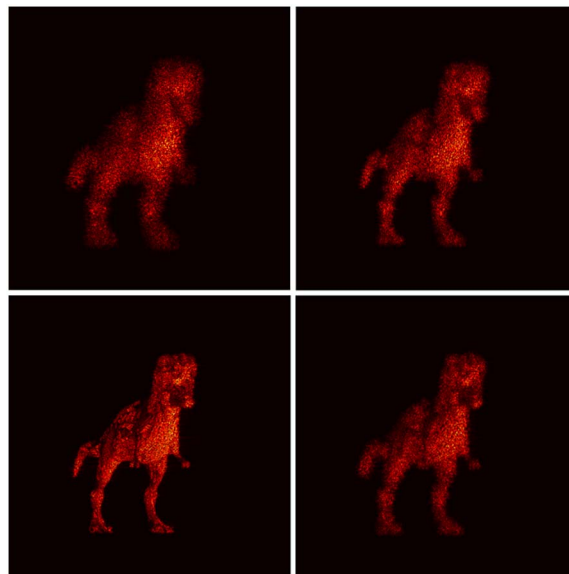

Fig. 23. (Color online) Numerical results of observation simulation. The observation simulation of CGH is performed. The observed holographic images taken at different focal planes are presented (View 4).

observed holographic object forms a continuously curved surface along the optical axis.

The triangular-mesh-based CGH synthesis algorithm provides very efficient and accurate holographic images of 3D objects with continuous spatial extent. With the advent of graphics processing units (GPUs), the efficient and fast computation of the angular spectrum of a tilted triangle became possible. The computational efficiency can be exponentially enhanced with scalable implementation of multiple GPU computing machines.

6. See-Through 3D Display Technologies

The ultimate goal of a 3D display may be generating a 3D image that is not distinguishable from a real object before we touch it. Of course, in the present status, the performance of 3D displays in expressing 3D images has not yet reached the level of providing a realistic 3D image. However, it is not enough just to raise the performance of a 3D display in order to meet the ultimate objective. For a seamless assimilation of a 3D image into the real world, the display device should provide a see-through feature to mediate the 3D image onto the real world, while the physical layout of the device is not noticeable to observers. Recently, augmented reality technology became an actively investigated research field that is to combine virtual and real physiological experiences [98,99]. In augmenting the visual sense of a user, the objective of an augmented reality field is the same as the final goal of 3D display—providing a perfect virtual image to the observer. In the early stage of augmented reality technology, a starting point for an augmented reality display device was implementing a see-through display with 2D virtual images. However, with the developments in electronic and optical devices, research has been conducted on implementing a see-through display with 3D virtual images. In this section, we will overview some important and recent reports on see-through 3D displays.

A. Head-Mounted See-Through Display

A head-mounted display (HMD) is a very early type of see-through display that uses a display device attached just in front of a human eye [100]. Despite many disadvantages from the head-worn requirement, it is still popular in some areas because of its easy and cheap implementation. Moreover, HMD can readily provide a 3D virtual image by binocular disparity. Because of its long history, it is the most mature technique among augmented reality displays, and plenty of investigations have been conducted considering the issues to be resolved. Nevertheless, further development is needed to commercialize see-through HMD devices. We will review some state-of-the-art HMD techniques and efforts to resolve issues in implementing see-through HMD devices.

To implement a light-weight and compact optical see-through HMD, it is preferred that a wedge-shaped prism is adopted to fold the optical path of a displayed image to an observer [101,102]. Figure 24 shows a typical configuration of an optical see-through HMD using a wedge-shaped prism. A wedge-shaped prism labeled 1 guides the light from a display panel to show a virtual image to an observer. Three surfaces of prism 1 are labeled a, b, and c, as shown in Fig. 24. Surface c should be treated with a thin film coating that shows transreflective characteristic. Surfaces b and c are designed for total internal reflection to occur at surface b for the rays entering through surface a. The reflected rays are reflected again at surface c by a transreflective characteristic, so the brightness of an image is decreased to a certain degree by the reflectance of surface c. The whole optical path of a displayed image through prism 1 is depicted as a solid arrow in Fig. 24. The shapes of the three surfaces should be designed to minimize the deformation of a displayed image shown to an observer. An auxiliary prism labeled 2 is attached to a wedge-shaped prism to achieve the see-through property of the system. If surface d is properly designed, the deformation of an image passing through the wedge-shaped prism, caused by the refraction at surfaces b and c, can be compensated by an auxiliary prism. The optical path of a transmitted see-through image is depicted as dashed arrows in Fig. 24. Because of the transreflective characteristic of surface c, the brightness of the transmitted image is also affected by the transmittance of surface c, and the transmittance should be determined considering applications and system specifications. With this configuration, a virtual image delivered to an observer by consecutive reflections inside a wedge-shaped prism can be overlaid on a real-world scene shown through a combination of two prisms. Adopting a free-form surface (FFS) provides a high degree of freedom in designing the shape of the surfaces of prisms, so the deformation of a virtual image and a real-world scene can be minimized. Cheng *et al.* introduced a systematic way to design surfaces of each prism using CODE V, and the result was verified by prototype implementation using FFS prisms [103]. They reported achievement of a
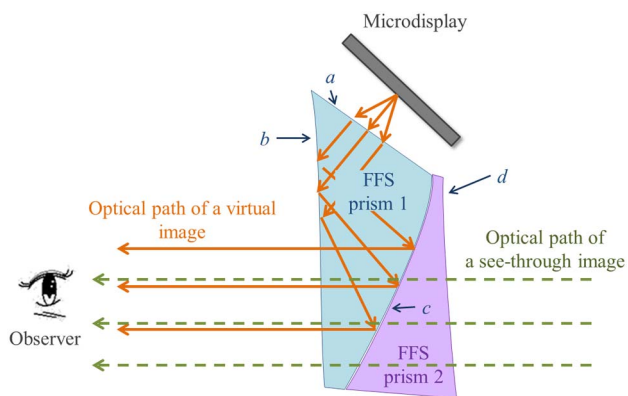

Fig. 24. (Color online) Typical configuration of an optical see-through HMD adopting a wedge-shaped prism.
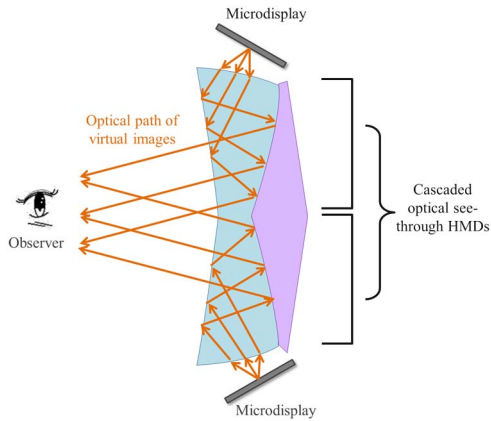
Fig. 25. (Color online) System configuration of an FOV-enhanced optical see-through HMD with tiled wedge-shaped prisms.

diagonal FOV of $53.5°$ and an f-number of 1.875, with an 8 mm exit pupil diameter and an 18.25 mm eye relief. Recently, they extended their work to provide a wider FOV by tiling the system shown in Fig. 24 [104]. Figure 25 shows the concept of the tiled see-through HMD system. The surface shape of each prism is designed to have a continuously cascaded FOV. Although the system needs a display device per each tiled prism, the FOV can easily be widened to a level that is not achievable by the tuning of one prism. They implemented the prototype with two FFS prisms tiled side by side, and the FOV of the prototype was widened to $82° × 32°$ with a small overlapping FOV to remove the vignetting effects at the transition region.

The optical see-through HMD using wedge-shaped prism shows that the entire system can be light weight and compact. However, the optical path of a virtual image is usually on-axis when it enters the observer's pupil after consecutive reflections inside a wedge-shaped prism. Instead of using such a configuration, a tilted optical combiner that has optical power can be used to implement an off-axis configuration. Figure 26 shows the layout of one of the
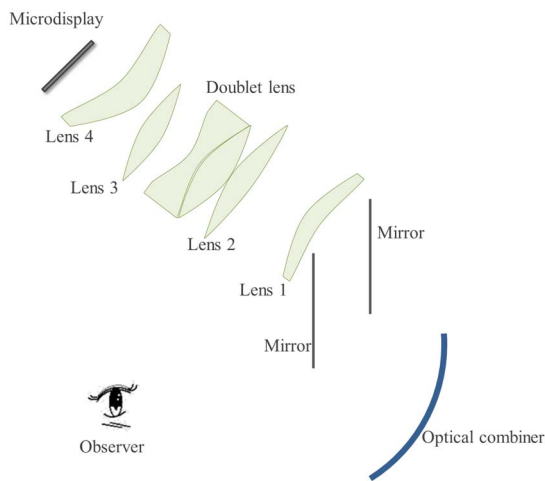
state-of-the-art systems with the off-axis configuration proposed by Zheng *et al.* [105]. Comparing with the on-axis configuration, the off-axis configuration has an advantage in that it can avoid the ghost image caused by multiple reflections inside the combiner.

One of the difficulties in mediating a virtual image to the real world with the optical see-through HMD is that a virtual image cannot occlude the real world when it is considered to be located between an observer and the real-world scene. The usual way to resolve the occlusion problem is to adopt an active LC mask to block rays from the real-world scene that coincide with a virtual image [106,107]. Kiyokawa *et al.* conducted a series of work on implementing the optical see-through HMD free from such an occlusion problem [108–111]. They also adopted an LC mask to selectively block the rays from the real world, but they were concerned about a problem where the real world and the LC mask cannot be in focus simultaneously because of a large difference in their locations. To resolve such a problem, the LC mask was located between two symmetrically located convex lenses with the same specifications as shown in Fig. 27(a). With the configuration shown in Fig. 27(a), an image of the LC mask is located at infinity, so the LC mask and the real-world scene are nearly in focus, while the real-world scene is maintained without lateral or transverse scaling. However, there are some disadvantages in adopting

Fig. 26. (Color online) Layout of an off-axis projection optical see-through HMD system.
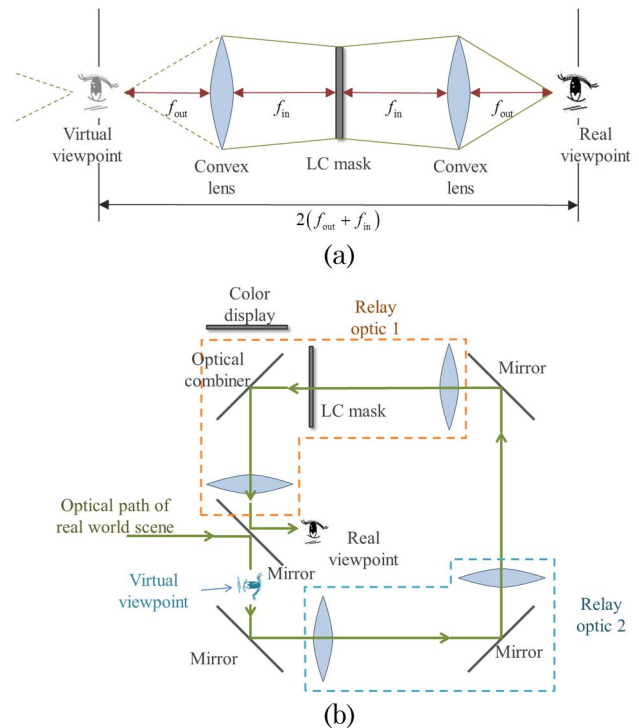

(a)

(b)

Fig. 27. (Color online) Configuration to resolve an occlusion problem in an optical see-through HMD. (a) Creation of occlusion with an LC mask. f_{in} and f_{out} are the inner and outer focal lengths of the convex lenses, respectively. (b) Ring-shaped structure of the entire system to compensate the shifted viewpoint and the inverted real-world scene.

the configuration shown in Fig. 27(a): The viewpoint of an observer is shifted by an offset of $2(f_{out} + f_{in})$. Hence, discomfort may arise by a mismatch between real and virtual viewpoints; the upside-down image of the real-world scene is shown to the observer. In their recent work, Kiyokawa *et al.* implemented a ring-shaped system, as shown in Fig. 27(b), to resolve these issues [111]. The rays from the real-world scene pass along a ring-shaped structure before being shown to the observer, and the optical path is depicted as a solid arrow. The relay optics labeled 2 in Fig. 27(b) inverts the real-world scene to compensate the upside-down problem of the configuration in Fig. 27(a). Then the part of the system labeled 1, which is the same as the configuration shown in Fig. 27(a), blocks selectively the rays from the real-world scene to provide proper occlusion. A virtual image displayed on the display device is mediated to the masked real-world image without the upside-down problem by the optical combiner before reaching an observer. The ring-shaped structure shifts the virtual viewpoint of an observer to the location where an offset to the exit pupil of the system becomes the same as the real viewpoint, so the mismatch between the real and virtual viewpoints is also resolved. The investigation using the implemented prototype based on this configuration reported that more than 75% of people felt an enhanced sense of the presence of virtual objects.

Most of the optical see-through HMDs simply combine a virtual image displayed on the display device, which is usually located near an observer's eye. When the point of interest of an observer is at a distant object in the real world, the accommodation to a near virtual image and a distant real object has a large difference, so it is difficult to provide a clear view of the combined real and virtual images. Introducing a varifocal or multifocal device for displaying a virtual image may resolve such a problem by shifting the image plane of a virtual image to a location where the point of interest of an observer is located [112,113]. The major problem in the varifocal display is that it is usually implemented by a time-multiplexed mechanical motion, so the stability of a system is not guaranteed and even flicker can occur in the displayed image. Another approach to resolving this issue is to project pixels of a virtual image directly on the retina of an observer's eye with a scanned laser beam [114]. However, the quality of an image displayed by a scanning laser beam is not yet compatible to the ordinary display device. Recently, Liu *et al.* reported an interesting system that implements a varifocal feature with an electronically controllable liquid lens [115]. In the implemented prototype, the liquid lens has a capability to vary optical power from −5 to 20 diopters by applying an AC voltage. Combined with a spherical mirror, as shown in Fig. 28, a displayed virtual image can be shifted to provide focus cues continuously from optical infinity to as close as 8 diopters without any mechanical motion. However, if multiple virtual
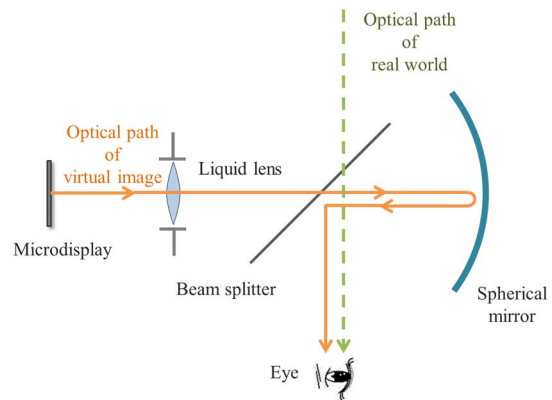

Fig. 28. (Color online) Accommodation-cue-addressable system using a liquid lens for a varifocal feature.

images with different locations are to be displayed, the liquid lens should address different optical powers simultaneously by time multiplexing. The operating speed of the liquid lens is not so fast yet, so Liu *et al.* reported that their implementation could address two different focal planes up to the speed of 21.25 Hz, which can cause a flickering to the HVS. Further developments in electronic devices are required to address multiple focal planes without flickering. Hence, it is still a challenge to resolve the accommodation mismatch problem in optical see-through HMDs.

B. Projection-Type See-Through 3D Display Technologies

Despite its long history, the see-through display based on HMD has many drawbacks that make it difficult to be accepted as a commercial product. Basically, the head-worn type limits the scenario of usage significantly because the displayed contents can be delivered to only one user who wears the device. Also, its use in the outdoors is also inconvenient because it requires users to always carry and wear the device when they want to enjoy the contents. Even safety issues can arise from the heavy weight and limited FOV of the complicated structure. Hence, HMD can be used only for very limited applications where the disadvantage of its head-worn nature is not a big issue. Instead, the projection-type see-through display is considered to be one viable candidate for implementing see-through display. The early implementation of projection-type see-through displays was simply to adopt a large-sized optical combiner as a screen and to project a virtual image on the optical combiner [116]. A transreflective glass is the most popular option for the optical combiner because it shows a clear see-through view of the real-world scene. Although not much time has passed since the projection-type see-through display adopting a transreflective glass became a popular research topic, it is already in the commercial market. Especially, the automobile industry has been very active in adopting it as a head-up display (HUD) on windshields. Therefore, the issues that have arisen from nonflat transreflective glass have also been explored in this

area [117,118]. Sometimes a partially diffusive screen is also adopted for the optical combiner to enhance the FOV and brightness of a projected virtual image. Although it has the drawback that an image of the real world becomes blurred by a diffusive characteristic, it is sometimes preferred to a beam splitter because of its wide viewing angle. Other than using a simple diffusive screen, some interesting ideas have been invented to implement a partially diffusive characteristic that can be used for an optical combiner [119–122]. One is an immaterial screen that is constructed by a flow of particles, such as dry fog, which is protected by a large nonturbulent airflow [119]. It is unique in that the observer can walk through the screen while the projected virtual image is well expressed by the scattering of particles. The other idea is to use water drops as a partially diffusive screen [120]. Because each water drop can be considered a tiny fish-eye lens, water drops show a scattering property for the projected image. The usefulness of these unique approaches has been investigated for various applications by many researchers [121,122]. We will review some recent technologies to implement a see-through 3D display based on the methods used for projection-type augmented reality displays.

The simplest way to implement a see-through display capable of providing a 3D virtual image is to use transreflective glass to combine a 3D image from a conventional 3D display with a real-world scene. One challenge in this configuration is that a real-world scene is usually very far from the observer in many situations. Hence, the adopted 3D display should be able to express a 3D image located far from the observer, but ordinary autostereoscopic displays do not provide such long distance 3D images. Takaki *et al.* introduced a super-multiview (SMV) display system for 3D display in a see-through display to overcome such a problem [123]. An SMV display is one kind of a multiview display that limits the width of each viewing zone to be less than the diameter of the eye pupil [124]. It is considered that a SMV display can provide an exact accommodation cue to a displayed 3D image and also a smooth motion parallax. Figure 29(a) shows the system configuration proposed by Takaki *et al.* The SMV display was implemented by a combination of a slanted lenticular lens display and a projection lens. Although the application for a windshield display was assumed in their investigation, they used a flat transreflective mirror as an optical combiner to exclude the prewarping issue in their considerations. As shown in Fig. 29(b), the viewing zone of a slanted lenticular lens array is imaged by a projection lens and the width of the entire viewing zone is reduced. Hence, the pitch of each viewing zone can be reduced to a desired level—less than the diameter of a pupil of an eye—if the parameters of the configuration are properly determined. Takaki *et al.* reported that their prototype provides 36 viewing zones with a pitch of 3.61 mm for each and it is possible to demon-
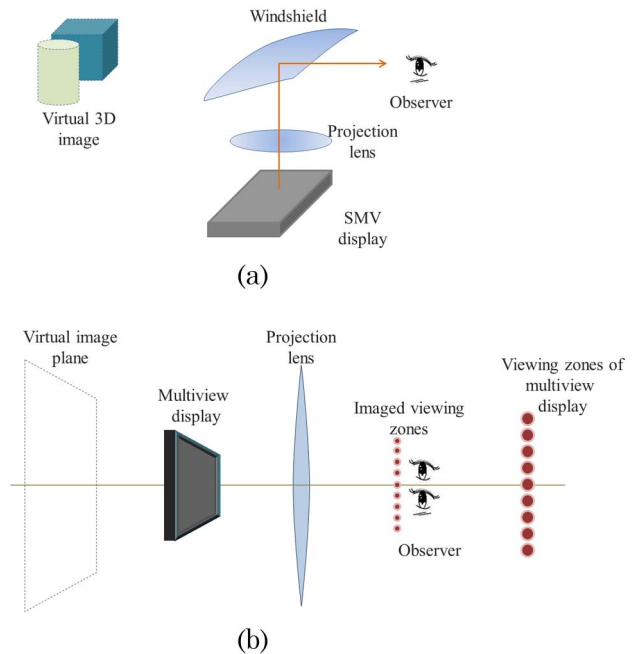

Fig. 29. (Color online) See-through 3D display system that adopts SMV display. (a) Conceptual diagram of a system configuration. (b) Implementation of SMV feature with reduced pitch of each viewing zone by a projection lens.

strate a continuous motion parallax for a 3D virtual image located 5–50 m from the observer. Although the see-through display combining an ordinary 3D display with a real-world scene by a transreflective mirror is intuitive and can express even a far virtual image with a SMV configuration, the entire system is bulky and the size of the displayed image is limited by the size of the incorporated 3D display. In addition, although it adopted a transreflective glass from a projection-type see-through display, it cannot be implemented as a projection type. In the following subsections, we will introduce some projection-type see-through 3D displays based on a diffusive screen.

A projection-type see-through display adopting a diffusive screen basically has difficulty in providing a 3D image because the image plane of a projected virtual image is fixed on the surface of the screen. Recently, Lee *et al.* proposed a system that introduces a depth-fused display (DFD) feature to show a 3D image with a diffusive screen [125]. DFD is one of the 3D display techniques that can provide 3D depth perception to an observer wearing no special apparatus with 2D images on two or more overlapping transparent screens—but generally two screens are enough [126]. The observer must be located at the position where identically rendered 2D images displayed on transparent screens are superimposed. Then the depth can be perceived pixel by pixel from superimposed 2D images by varying the luminance of each pixel of each 2D image. If a pixel on the frontal screen is more luminous, the pixel will be perceived to be near the observer. In contrast, if a pixel on the back screen is more luminous, the pixel will be perceived to be far from the observer. It is considered that
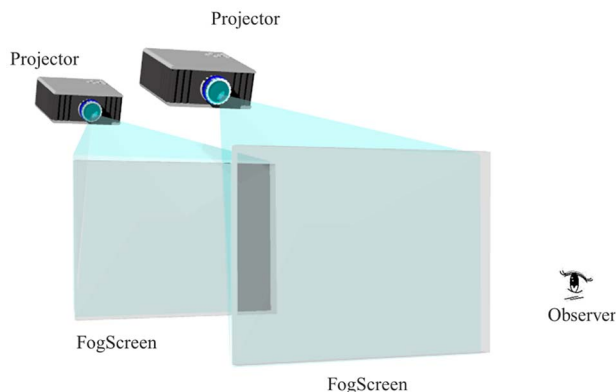
Fig. 30. (Color online) See-through 3D display adopting DFD feature to show a 3D image with a diffusive screen.

Fig. 31. (Color online) Concept of a multilayered display with water drops. (a) Side view. (b) Top view.

an accommodation cue to fused depth perception is free from the visual fatigue problems of stereoscopic displays [127]. Lee *et al.* adopted two fog screens for diffusive screens, and they stacked two screens, as shown in Fig. 30. They demonstrated that the two superimposed projected images can express a 3D volume in between two screens, and the fixed single viewpoint of a DFD was overcome by using head tracking. By using this technique, it is possible to implement a projection-type see-through display that can provide a 3D virtual image mediated to the real world. It is even possible to walk through the screen because it is immaterial, and it can give a degree of freedom in a scenario of usage. However, the range where a 3D virtual image can be expressed is limited only between two screens, and the use of a diffusive screen affects the quality of a real-world scene.

One unique approach in implementing a projection-type see-through display with a 3D virtual image is to use multiple water drop screens as diffusive screens, as proposed by Barnum *et al.* [128]. Instead of using a DFD scheme, they tried to implement multiple image planes to express a virtual 3D image. Simply stacking multiple water drop screens cannot provide independent image planes because the back plane image is diffused again by the frontal diffusive screens. To address each image plane independently, time differential projection to each water drop screen is utilized. Unlike other diffusive screens, each particle of a water drop screen moves continuously and is controllable. Hence, it is possible to realize a time differential projection with the concept shown in Fig. 31. As shown in Fig. 31(a), if a water drop from each drop emitter has a slight time difference, it is possible to independently project a water drop from each emitter with an obliquely located projector. If the projected image and the drop emitters are properly synchronized, water drops from each drop emitter can be addressed independently and the afterimage of water drops can show a 2D image on each plane. In their implementation, Barnum *et al.* used a camera for the synchronization by calculating the locations of drops from a captured image. With this implementation, they realized a
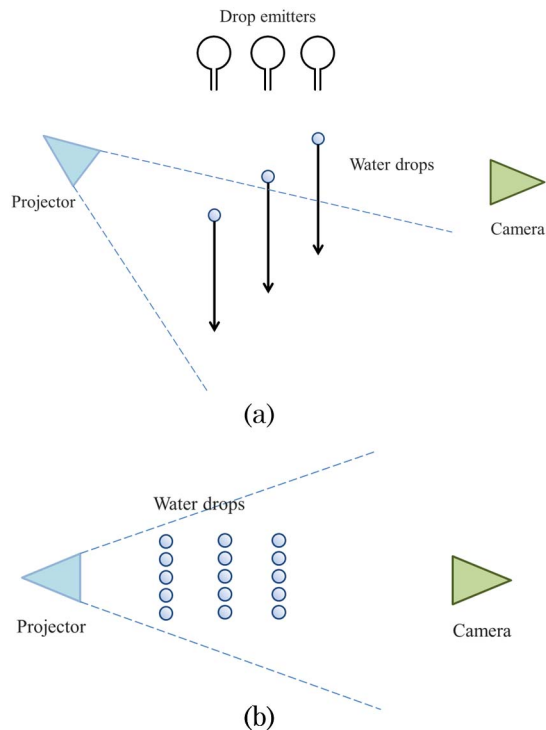
system with three independently addressable water drop screens and 10 drops per second for each. Although they demonstrated only stacked 2D images, the DFD feature is readily applicable for each adjacent screen pair, so it is expected that the continuously expressed 3D virtual image can be successfully mediated with a real-world scene by using this system. However, this pioneering work is very sensitive to timing and alignment, so further improvement is needed to resolve the stability issue for a commercial product.

C. See-Through 3D Display Using a Holographic Optical Element

The see-through display systems discussed so far demand optical combiners in any form to mediate a virtual image to a real-world scene. The design and implementation of such an optical combiner is not easy, and sometimes it induces limitation in the performance of an entire system. A holographic optical element (HOE) can be a good alternative to implement a required optical combiner in a see-through display because holographic recording materials have many useful characteristics: they are ordinarily very clear and transparent even after an optical element is recorded, they are flexible, so there is a high degree of freedom in designing the shape of a system, and they are very thin and lightweight. Although it is popular to adopt HOEs for optical see-through HMDs [129], we will investigate only the cases where an HOE is applied to a projection-type see-through display system.
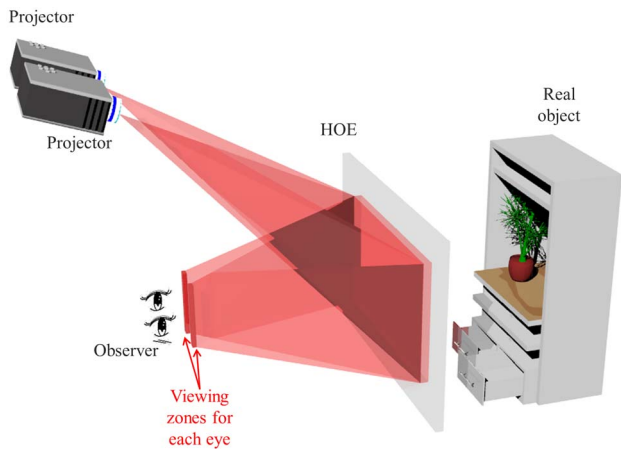
Fig. 32. (Color online) Autostereoscopic see-through display adopting an HOE and two projectors.

The difficulty in constructing a projection-type see-through display system using a diffusive screen was that the rays scattered on the diffusive screen lose their directivity, so the left and right eyes cannot see different images. This means that there is no parallax in a displayed virtual image. An HOE can be an alternative to an optical screen that can give a freely designed directivity to a projected image. Olwal *et al.* proposed an autotstereoscopic see-through system adopting an HOE as a screen that can show different virtual images to the left and right eyes of an observer [130]. In their implementation, as shown in Fig. 32, an HOE is recorded to focus projected images from two projectors to different locations that are to be viewing zones for the two eyes of an observer. If the viewing zones are properly designed, each eye of the observer views a virtual image coming from a different projector, and a 3D image can be perceived by binocular disparity. As a proof of concept, Olwal *et al.* implemented a system that has only two viewing zones with an HOE recorded on an ultrafine grain silver–halide emulsion with a size of 30 cm × 40 cm. Therefore, an autostereoscopic virtual image can be viewed only at a single fixed position and the implemented system provides only a monochrome image. Theoretically, the concept could be extended to a full-color multiview system by recording an HOE to have multiple viewing zones. However, it would require multiple projectors that should be precisely aligned and the diffraction efficiency of the HOE will decrease as the number of viewing zones increases. It will be worthy to verify a multiview concept by a real implementation to check usability and limitations.

Takahashi *et al.* proposed an HOE that performs a lenticular-lens-like function in their series of work to show an autostereoscopic virtual image with a single projector [131–134]. Figure 33(a) shows a configuration of their proposed HOE structure, which is composed of an array of identical grating cells. Each column of the grating cell array coincides with each line of a lenticular lens. The concept of a grating cell was adopted to increase the horizontal angular
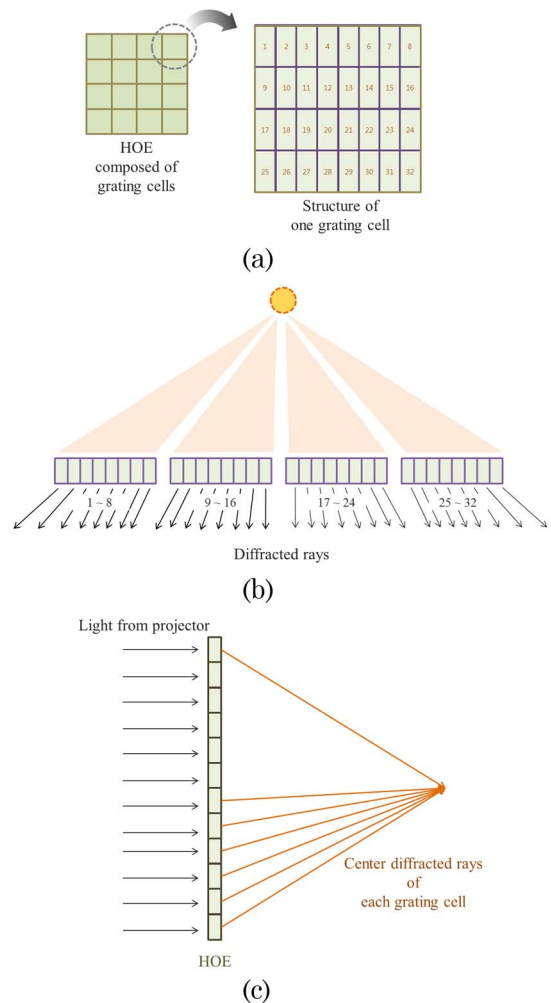
Fig. 33. (Color online) See-through 3D display adopting a lenticular-lens-like HOE. (a) Structure of the HOE and grating cell. (b) Directions of rays diffracted by one grating cell. (c) Wide-viewing-angle implementation with a curved-lens-like recording of HOE.

resolution at the cost of decreased spatial resolution in the vertical direction. Each grating cell is designed to diffract incident rays to 32 horizontal directions,

Fig. 34. (Color online) See-through 3D display system based on CHMA.

Fig. 35. (Color online) Sampling and reconstruction processes of outlined technologies: (a) integral imaging, (b) multiview display, (c) holography, and (d) see-through 3D display.

as shown in Fig. 33(b). Therefore, the HOE can be considered a lenticular lens that provides 32 multiple views in the horizontal direct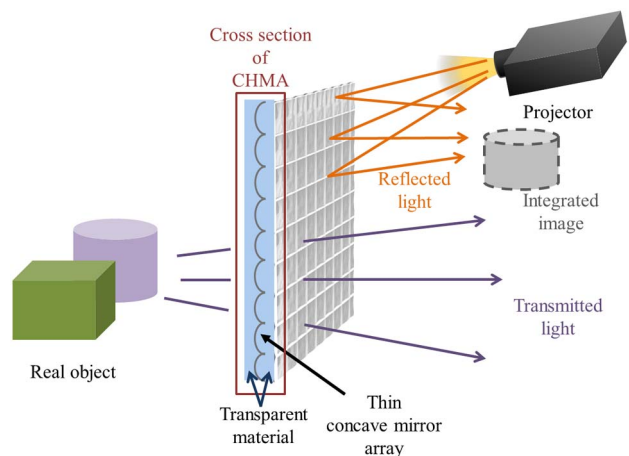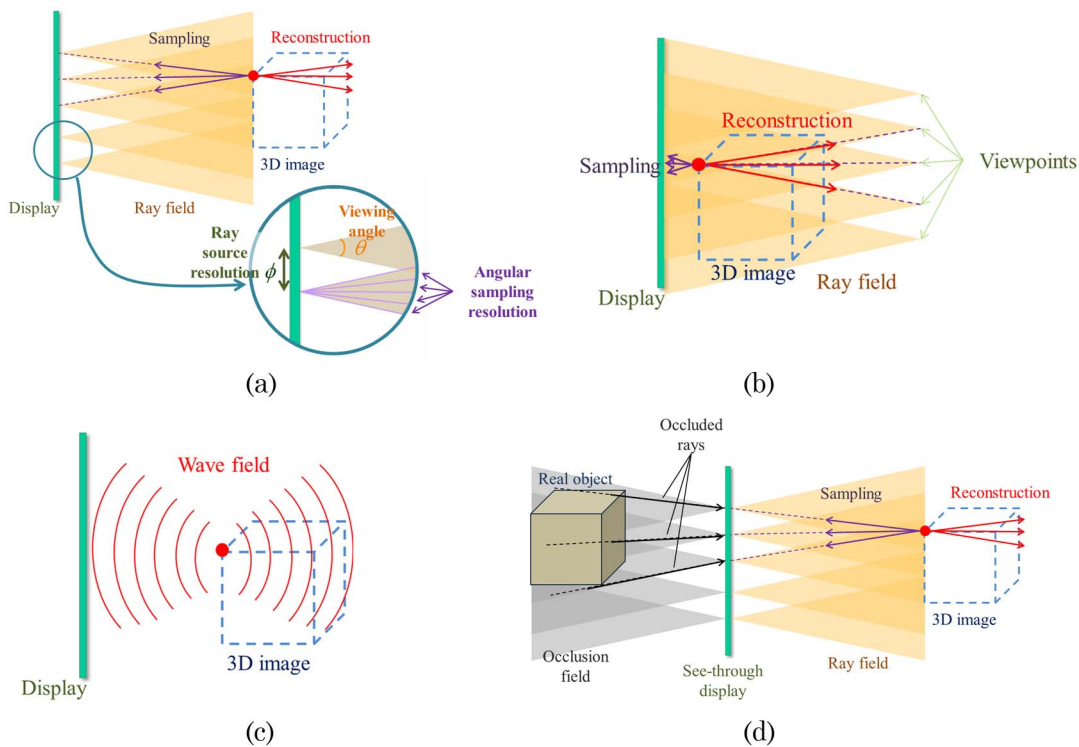ion. To display a 3D virtual image using the recorded HOE, a properly calculated image is projected to the HOE and it is diffracted to 32 directions. In an observer's viewpoint, each grating cell of the HOE is recognized as one pixel of a displayed virtual image and the observer can view 32 different images by changing viewing locations. Takahashi *et al.* also extended their work to realize a curved-lens-array-like configuration to increase the viewing angle of the system [134]. Implementing a physical optical structure that shows a curved lens array configuration results in a bulky system and fabrication is usually difficult and expensive. However, it is possible to construct such a feature as a flat and thin HOE because the direction of diffraction of each grating cell can be freely designed. When the diffracted ray at the center of each grating cell is designed to converge into a certain point in the horizontal direction, as shown in Fig. 33(c), the desired characteristic can be implemented. Takahashi *et al.* reported that the viewing angle was increased from 42° to 74° by adopting such curved-lens-array-like feature.

D. See-Through 3D Display Using a Concave Half-Mirror Array

Our group recently proposed a new optical structure called a concave half-mirror array (CHMA) whose external appearance is a transparent plate [135]. Inside a structure, there is an array of concave mirrors with a transreflective characteristic, as shown

in Fig. 34. The CHMA does not affect the optical path of transmitted rays, while the optical path of reflected rays are affected by the concave mirror array structure inside the CHMA. Hence, the CHMA acts as different optical elements on reflected and transmitted light. Figure 34 shows a system configuration that can implement a projection-type see-through 3D display based on a CHMA. As a CHMA is only a transparent plate to transmitted rays, it shows a see-through characteristic to a real-world scene. Because a concave mirror array is a direct alternative to a lenslet array, a setup incorporating a projector can create a virtual 3D image by reflection of a projected elemental image. The CHMA is the only possible method existing, except for an HOE, that can mediate an autostereoscopic 3D image to a real-world scene by projection. The fabrication method presented in [135] is not appropriate for use as a see-through display because the implementation cannot be shown as a perfect transparent plate to transmitted rays. Hence, the fabrication method should be further investigated to apply a CHMA to a see-through 3D display.

7. Conclusion

It is hard to predict which one of the outlined technologies will be the next to be a commercial product. Although the result depends completely on the demands of the market, most market research forecasts that autostereoscopic display and holography will be commercialized in sequence. Those technologies can be categorized according to principles underlying their sampling and reconstruction

processes. As shown in Fig. 35, autostereoscopic display is a method to replicate a ray field created by 3D objects. There are a set of digitized rays that an autostereoscopic display can express and a ray field of 3D objects is sampled under that set of rays. The only difference between integral imaging and a multiview display, such as lenticular lenses, exists in the sampling process. Integral imaging samples a ray field from ray source locations, while a multiview display samples from predetermined viewpoints, as compared in Figs. 35(a) and 35(b). Then such a digitized ray field is reconstructed when an autostereoscopic display operates. Therefore, autostereoscopic display is more appropriate to digital devices because various digital signal processing techniques developed so far can be applied directly. In contrast, holography is a technique to record and reconstruct the wave field of a given 3D image and it shows a perfect reconstruction of a 3D image in principle. However it is more difficult to represent an analog wave field with a digital display device; hence, its implementation is considered more challenging than autostereoscopic display.

Despite its easier implementation, autostereoscopy still needs further development in display devices and optics because various quality factors of the reconstructed ray field are severely limited by the system parameters of display devices and optics. Representative quality factors of a ray field are ray source resolution, angular sampling resolution, and viewing angle, as shown in Fig. 35(a). However, with the present status of display device and optics, a satisfactory 3D image cannot be reconstructed by autostereoscopic display because only part of the ray field can be expressed.

See-through 3D display presents a mixture of the ray fields of both the real-world and the virtual 3D image. It is more future technology and further development is needed to resolve some critical issues. One important issue is the occlusion problem that was described in Subsection 6.A. Without appropriate occlusion of the real world, a reconstructed 3D image will suffer from a translucent problem. However, in dealing with a 3D image, a ray-based mask should be realized instead of a simple 2D mask. Hence, it is necessary to provide a so-called "occlusion field" in the real-world side and no methods have yet been proposed to provide an occlusion field, to the best of our knowledge. If implemented, it may be similar in principle with ray-field generation. A difficulty in implementing a ray-based occlusion field is that there is the same limitation as in a ray-field-based approach. This means that an occlusion field can address only a part of a ray field from a real-world scene and it can affect the quality of the real-world scene. To avoid degradation in a real-world scene, the occlusion field should cover a sufficiently large part of the ray field, which requires further improvement in digital display devices than does autostereoscopic display.

In conclusion, it is still early to expect a commercial product based on autostereoscopic or holographic display devices. However, we believe that a commercial product will appear in the market shortly because the technical issues discussed so far will be resolved in the end with continuing research effort, and a value chain of the 3D display industry is already working.

References

1. C. Wheatstone, "Contributions to the physiology of vision. Part the first. On some remarkable, and hitherto unobserved, phenomena of binocular vision," Philos. Trans. R. Soc. London **128**, 371–394 (1838).
2. T. Inoue and H. Ohzu, "Accommodation responses to stereoscopic three-dimensional display," Appl. Opt. **36**, 4509–4515 (1997).
3. F. L. Kooi and A. Toet, "Visual comfort of binocular and 3D displays," Displays **25**, 99–108 (2004).
4. S. S. Kim, B. H. You, H. Choi, B. H. Berkeley, and N. D. Kim, "World's first 240 Hz TFT-LCD technology for full-HD LCD-TV and its application to 3D display," in *SID International Symposium Digest of Technical Papers* (Society for Information Display, 2009), Vol. 40, pp. 424–427.
5. D.-S. Kim, S.-M. Park, J.-H. Jung, and D.-C. Hwang, "New 240 Hz driving method for Full HD and high quality 3D LCD TV," in *SID International Symposium Digest of Technical Papers* (Society for Information Display, 2010), Vol. 41, pp. 762–765.
6. H. Kang, S.-D. Roh, I.-S. Baik, H.-J. Jung, W.-N. Jeong, J.-K. Shin, and I.-J. Chung, "A novel polarizer glasses-type 3D displays with a patterned retarder," in *SID International Symposium Digest of Technical Papers* (Society for Information Display, 2010), Vol. 41, pp. 1–4.
7. S.-M. Jung, Y.-B. Lee, H.-J. Park, S.-C. Lee, W.-N. Jeong, J.-K. Shin, and I.-J. Chung, "Improvement of 3-D crosstalk with over-driving method for the active retarder 3-D displays," in *SID International Symposium Digest of Technical Papers* (Society for Information Display, 2010), Vol. 41, pp. 1264–1267.
8. S. T. de Zwart, W. L. Ijzerman, T. Dekker, and W. A. M. Wolter, "A 20 in. switchable auto-stereoscopic 2D/3D display," in *Proceedings of International Display Workshops* (Society for Information Display, 2004), pp. 1459–1460.
9. G. J. Woodgate and J. Harrold, "A new architecture for high resolution autostereoscopic 2D/3D displays using free-standing liquid crystal microlenses," in *SID International Symposium Digest of Technical Papers* (Society for Information Display, 2005), Vol. 36, pp. 378–381.
10. H.-K. Hong, S.-M. Jung, B.-J. Lee, H.-J. Im, and H.-H. Shin, "Autostereoscopic 2D/3D switching display using electric-field-driven LC lens (ELC lens)," in *SID International Symposium Digest of Technical Papers* (Society for Information Display, 2008), Vol. 39, pp. 348–351.
11. C.-W. Chen, Y.-C. Huang, and Y.-P. Huang, "Fast switching Fresnel liquid crystal lens for autostereoscopic 2D/3D display," in *SID International Symposium Digest of Technical Papers* (Society for Information Display, 2010), Vol. 41, pp. 428–431.

12. A. Takagi, T. Saishu, M. Kashiwagi, K. Taira, and Y. Hirayama, "Autostereoscopic partial 2-D/3-D switchable display using liquid-crystal gradient index lens," in *SID International Symposium Digest of Technical Papers* (Society for Information Display, 2010), Vol. 41, pp. 436–439.

13. H. J. Lee, H. Nam, J. D. Lee, H. W. Jang, M. S. Song, B. S. Kim, J. S. Gu, C. Y. Park, and K. H. Choi, "A high resolution autostereoscopic display employing a time division parallax barrier," in *SID International Symposium Digest of Technical Papers* (Society for Information Display, 2006), Vol. 37, pp. 81–84.

14. G. Hamagishi, "Analysis and improvement of viewing conditions for two-view and multi-view 3D displays," in *SID International Symposium Digest of Technical Papers* (Society for Information Display, 2009), Vol. 40, pp. 340–343.

15. G. Lippmann, "La photographie integrale," C. R. Acad. Sci. **146**, 446–451 (1908).

16. F. Okano, H. Hoshino, J. Arai, and I. Yuyama, "Real-time pickup method for a three-dimensional image based on integral photography," Appl. Opt. **36**, 1598–1603 (1997).

17. B. Lee, J.-H. Park, and S.-W. Min, "Three-dimensional display and information processing based on integral imaging," in *Digital Holography and Three-Dimensional Display* T.-C. Poon, ed. (Springer, 2006), Chap. 12, pp. 333–378.

18. S.-W. Min, J. Kim, and B. Lee, "New characteristic equation of three-dimensional integral imaging system and its applications," Jpn. J. Appl. Phys. **44**, L71–L74 (2005).

19. J.-H. Park, K. Hong, and B. Lee, "Recent progress in three-dimensional information processing based on integral imaging," Appl. Opt. **48**, H77–H94 (2009).

20. Y. Kim, S.-G. Park, S.-W. Min, and B. Lee, "Integral imaging system using a dual-mode technique," Appl. Opt. **48**, H71–H76 (2009).

21. J. Hahn, Y. Kim, and B. Lee, "Uniform angular resolution integral imaging display with boundary folding mirrors," Appl. Opt. **48**, 504–511 (2009).

22. Y. Takaki, K. Tanaka, and J. Nakamura, "Super multi-view display with a lower resolution flat-panel display," Opt. Express **19**, 4129–4139 (2011).

23. M. Okui, M. Kobayashi, J. Arai, and F. Okano, "Moiré fringe reduction by optical filters in integral three-dimensional imaging on a color flat-panel display," Appl. Opt. **44**, 4475–4483 (2005).

24. Y. Kim, G. Park, J.-H. Jung, J. Kim, and B. Lee, "Color moiré pattern simulation and analysis in three-dimensional integral imaging for finding the moiré-reduced tilted angle of a lens array," Appl. Opt. **48**, 2178–2187 (2009).

25. Y. Kim, S.-G. Park, S.-W. Min, and B. Lee, "Projection-type integral imaging system using multiple elemental image layers," Appl. Opt. **50**, B18–B24 (2011).

26. M. Kawakita, H. Sasaki, J. Arai, F. Okano, K. Suehiro, Y. Haino, M. Yoshimura, and M. Sato, "Geometric analysis of spatial distortion in projection-type integral imaging," Opt. Lett. **33**, 684–686 (2008).

27. F. Okano, J. Arai, and M. Kawakita, "Wave optical analysis of integral method for three-dimensional images," Opt. Lett. **32**, 364–366 (2007).

28. X. Wang and H. Hua, "Theoretical analysis for integral imaging performance based on microscanning of a microlens array," Opt. Lett. **33**, 449–451 (2008).

29. J.-S. Jang and B. Javidi, "Improved viewing resolution of three-dimensional integral imaging by use of nonstationary micro-optics," Opt. Lett. **27**, 324–326 (2002).

30. H. Choi, S.-W. Min, S. Jung, J.-H. Park, and B. Lee, "Multiple-viewing-zone integral imaging using a dynamic barrier array for three-dimensional displays," Opt. Express **11**, 927–932 (2003).

31. B. Lee, S. Jung, and J.-H. Park, "Viewing-angle-enhanced integral imaging by lens switching," Opt. Lett. **27**, 818–820 (2002).

32. J.-S. Jang and B. Javidi, "Improvement of viewing angle in integral imaging by use of moving lenslet arrays with low fill factor," Appl. Opt. **42**, 1996–2002 (2003).

33. S. Jung, J.-H. Park, H. Choi, and B. Lee, "Wide-viewing integral three-dimensional imaging by use of orthogonal polarization switching," Appl. Opt. **42**, 2513–2520 (2003).

34. G. Park, J.-H. Jung, K. Hong, Y. Kim, Y.-H. Kim, S.-W. Min, and B. Lee, "Multi-viewer tracking integral imaging system and its viewing zone analysis," Opt. Express **17**, 17895–17908 (2009).

35. Y. Kim, J.-H. Park, S.-W. Min, S. Jung, H. Choi, and B. Lee, "A wide-viewing-angle integral 3D imaging system by curving a screen and a lens array," Appl. Opt. **44**, 546–552 (2005).

36. Y. Kim, J.-H. Park, H. Choi, S. Jung, S.-W. Min, and B. Lee, "Viewing-angle-enhanced integral imaging system using a curved lens array," Opt. Express **12**, 421–429 (2004).

37. D.-H. Shin, B. Lee, and E.-S. Kim, "Multidirectional curved integral imaging with large depth by additional use of a large-aperture lens," Appl. Opt. **45**, 7375–7381 (2006).

38. J.-H. Jung, K. Hong, G. Park, I. Chung, and B. Lee, "360-degree viewable cylindrical integral imaging system using three-dimensional/two-dimensional switchable and flexible backlight," J. Soc. Inf. Disp. **18**, 527–534 (2010).

39. S.-W. Min, J. Kim, and B. Lee, "Wide-viewing projection-type integral imaging system with an embossed screen," Opt. Lett. **29**, 2420–2422 (2004).

40. R. Martinez-Cuenca, H. Navarro, G. Saavedra, B. Javidi, and M. Martinez-Corral, "Enhanced viewing-angle integral imaging by multiple-axis telecentric relay system," Opt. Express **15**, 16255–16260 (2007).

41. G. Baasantseren, J.-H. Park, K.-C. Kwon, and N. Kim, "Viewing angle enhanced integral imaging display using two elemental image masks," Opt. Express **17**, 14405–14417 (2009).

42. H. Kim, J. Hahn, and B. Lee, "The use of a negative index planoconcave lens array for wide-viewing angle integral imaging," Opt. Express **16**, 21865–21880 (2008).

43. J.-Y. Jang, H.-S. Lee, S. Cha, and S.-H. Shin, "Viewing angle enhanced integral imaging display by using a high refractive index medium," Appl. Opt. **50**, B71–B76 (2011).

44. H. Liao, T. Dohi, and M. Iwahara, "Improved viewing resolution of integral videography by use of rotated prism sheets," Opt. Express **15**, 4814–4822 (2007).

45. Y. Kim, J. Kim, J.-M. Kang, J.-H. Jung, H. Choi, and B. Lee, "Point light source integral imaging with improved resolution and viewing angle by the use of electrically movable pinhole array," Opt. Express **15**, 18253–18267 (2007).

46. H. Liao, M. Iwahara, N. Hata, and T. Dohi, "High-quality integral videography using a multiprojector," Opt. Express **12**, 1067–1076 (2004).

47. H. Liao, M. Iwahara, T. Koike, N. Hata, I. Sakuma, and T. Dohi, "Scalable high-resolution integral videography autostereoscopic display with a seamless multiprojection system," Appl. Opt. **44**, 305–315 (2005).

48. J.-S. Jang, F. Jin, and B. Javidi, "Three-dimensional integral imaging with large depth of focus by use of real and virtual image fields," Opt. Lett. **28**, 1421–1423 (2003).

49. J.-H. Park, S. Jung, H. Choi, and B. Lee, "Integral imaging with multiple image planes using a uniaxial crystal plate," Opt. Express **11**, 1862–1875 (2003).

50. J.-S. Jang and B. Javidi, "Large depth-of-focus time-multiplexed three-dimensional integral imaging by use of

lenslet with nonuniform focal lengths and aperture sizes," Opt. Lett. **28**, 1924–1926 (2003).

51. H. Choi, J.-H. Park, J. Hong, and B. Lee, "Depth enhanced integral imaging with a stepped lens array or a composite lens array for three-dimensional display," Jpn. J. Appl. Phys. **43**, 5330–5336 (2004).

52. S. Jung, J. Hong, J.-H. Park, Y. Kim, and B. Lee, "Depth-enhanced integral-imaging 3D display using different optical path lengths by polarization devices or mirror barrier array," J. Soc. Inf. Disp. **12**, 461–467 (2004).

53. J. Hong, J.-H. Park, S. Jung, and B. Lee, "Depth enhanced integral imaging by use of optical path control," Opt. Lett. **29**, 1790–1792 (2004).

54. H. Choi, Y. Kim, J.-H. Park, J. Kim, S.-W. Cho, and B. Lee, "Layered-panel integral imaging without the translucent problem," Opt. Express **13**, 5769–5776 (2005).

55. Y. Kim, J.-H. Park, H. Choi, J. Kim, S.-W. Cho, Y. Kim, G. Park, and B. Lee, "Depth-enhanced integral imaging display system with electrically variable image planes using polymer-dispersed liquid-crystal layers," Appl. Opt. **46**, 3766–3773 (2007).

56. S.-W. Min, M. Hahn, J. Kim, and B. Lee, "Three-dimensional electro-floating display system using an integral imaging method," Opt. Express **13**, 4358–4369 (2005).

57. J. Kim, S.-W. Min, Y. Kim, and B. Lee, "Analysis on viewing characteristics of integral floating system," Appl. Opt. **47**, D80–D86 (2008).

58. J. Kim, S.-W. Min, and B. Lee, "Viewing window expansion of integral floating display," Appl. Opt. **48**, 862–867 (2009).

59. J. Kim, S.-W. Min, and B. Lee, "Viewing region maximization of an integral floating display through location adjustment of viewing window," Opt. Express **15**, 13023–13034 (2007).

60. J. Kim, S.-W. Min, and B. Lee, "Floated image mapping for integral floating display," Opt. Express **16**, 8549–8556 (2008).

61. H. Kakeya, "Autostereoscopic display with real-image virtual screen and light filters," Proc. SPIE **4660**, 349–357 (2002).

62. H. Kakeya, "MOEVsion: simple multiview display with clear floating image," Proc. SPIE **6490**, 64900J (2007).

63. H. Choi, Y. Kim, J. Kim, S.-W. Cho, and B. Lee, "Depth- and viewing-angle-enhanced 3-D/2-D switchable display system with high contrast ratio using multiple display devices and a lens array," J. Soc. Inf. Disp. **15**, 315–320 (2007).

64. Y. Kim, H. Choi, J. Kim, S.-W. Cho, Y. Kim, G. Park, and B. Lee, "Depth-enhanced integral imaging display system with electrically variable image planes using polymer-dispersed liquid crystal layers," Appl. Opt. **46**, 3766–3773 (2007).

65. H. Choi, S.-W. Cho, J. Kim, and B. Lee, "A thin 3D-2D convertible integral imaging system using a pinhole array on a polarizer," Opt. Express **14**, 5183–5190 (2006).

66. S.-W. Cho, J.-H. Park, Y. Kim, H. Choi, J. Kim, and B. Lee, "Convertible two-dimensional–three-dimensional display using an LED array based on modified integral imaging," Opt. Lett. **31**, 2852–2854 (2006).

67. Y. Kim, H. Choi, S.-W. Cho, Y. Kim, J. Kim, G. Park, and B. Lee, "Three-dimensional integral display using plastic optical fibers," Appl. Opt. **46**, 7149–7154 (2007).

68. Y. Kim, J. Kim, Y. Kim, H. Choi, J.-H. Jung, and B. Lee, "Thin-type integral imaging method with an organic light emitting diode panel," Appl. Opt. **47**, 4927–4934 (2008).

69. J.-H. Jung, Y. Kim, Y. Kim, J. Kim, K. Hong, and B. Lee, "Integral imaging system using an electroluminescent film backlight for three-dimensional–two-dimensional convertibility and a curved structure," Appl. Opt. **48**, 998–1007 (2009).

70. H. Choi, J. Kim, S.-W. Cho, Y. Kim, J. B. Park, and B. Lee, "Three-dimensional–two-dimensional mixed display system using integral imaging with an active pinhole array on a liquid crystal panel," Appl. Opt. **47**, 2207–2214 (2008).

71. D. Gabor, "A new microscopic principle," Nature **161**, 777–778 (1948).

72. E. N. Leith and J. Upatnieks, "Reconstructed wavefronts and communication theory," J. Opt. Soc. Am. **52**, 1123–1130 (1962).

73. Y. N. Denisyuk, "Photographic reconstruction of the optical properties of an object in its own scattered field," Sov. Phys. Dokl. **7**, 543 (1962).

74. G. Lippmann, "La photographie des couleurs," C.R. Hebd. Seances Acad. Sci. **112**, 274–275 (1891).

75. A. W. Lohmann and D. Paris, "Binary Fraunhofer holograms generated by computer," Appl. Opt. **6**, 1739–1748 (1967).

76. J. W. Goodman and R. W. Lawrence, "Digital image formation from electronically detected holograms," Appl. Phys. Lett. **11**, 77–79 (1967).

77. J. Schmit and K. Creath, "Extended averaging technique for derivation of error-compensating algorithms in phase-shifting interferometry," Appl. Opt. **34**, 3610–3619 (1995).

78. I. Yamaguchi and T. Zhang, "Phase-shifting digital holography," Opt. Lett. **22**, 1268–1270 (1997).

79. J. Millerd, N. Brock, J. Hayes, M. North-Morris, M. Novak, and J. C. Wyant, "Pixelated phase-mask dynamic interferometer," Proc. SPIE **5531**, 304–314 (2004).

80. J. W. Goodman, *Introduction to Fourier Optics*, 3rd ed. (Roberts, 2004).

81. A. V. Oppenheim and J. S. Lim, "The importance of phase in signals," Proc. IEEE **69**, 529–541 (1981).

82. J. Hahn, H. Kim, Y. Lim, G. Park, and B. Lee, "Wide viewing angle dynamic holographic stereogram with a curved array of spatial light modulators," Opt. Express **16**, 12372–12386 (2008).

83. D. J. Brady, *Optical Imaging and Spectroscopy* (Wiley, 2009).

84. L. Onural, F. Yaraş, and H. Kang, "Digital holographic three-dimensional video displays," Proc. IEEE **99**, 576–589 (2011).

85. K. Maeno, N. Fukaya, O. Nishikawa, K. Sato, and T. Honda, "Electro-holographic display using 15 mega pixels LCD," Proc. SPIE **2652**, 15–23 (1996).

86. J. W. Goodman, *Speckle Phenomena in Optics: Theory and Applications* (Roberts, 2007).

87. P. J. van Heerden, "A new optical method of storing and retrieving information," Appl. Opt. **2**, 387–392 (1963).

88. N. Abramson, "Light-in-flight recording: high-speed holographic motion pictures of ultrafast phenomena," Appl. Opt. **22**, 215–232 (1983).

89. J. R. Fienup and J. J. Miller, "Aberration correction by maximizing generalized sharpness metrics," J. Opt. Soc. Am. A **20**, 609–620 (2003).

90. M. Stanley, R. W. Bannister, C. D. Cameron, S. D. Coomber, I. G. Cresswell, J. R. Hughes, V. Hui, P. O. Jackson, K. A. Milham, R. J. Miller, D. A. Payne, J. Quarrel, D. C. Scattergood, A. P. Smith, M. A. Smith, D. L. Tipton, P. J. Watson, P. J. Webber, and C. W. Slinger, "100 mega-pixel computer generated holographic images from active tiling–a dynamic and scalable electro-optic modulator system," Proc. SPIE **5005**, 247–258 (2003).

91. R. Haussler, S. Reichelt, N. Leister, E. Zschau, R. Missbach, and A. Schwerdtner, "Large real-time holographic displays: from prototypes to a consumer product," Proc. SPIE **7237**, 72370S (2009).

92. Y. Takaki and M. Yokouchi, "Speckle-free and grayscale hologram reconstruction using time-multiplexing technique," Opt. Express **19**, 7567–7579 (2011).

93. I. Yamaguchi and T. Zhang, "Phase-shifting digital holography," Opt. Lett. **22**, 1268–1270 (1997).

94. N. T. Shaked, B. Katz, and J. Rosen, "Review of three-dimensional holographic imaging by multiple-viewpoint-projection based methods," Appl. Opt. **48**, H120–H136 (2009).

95. J.-H. Park, M.-S. Kim, G. Baasantseren, and N. Kim, "Fresnel and Fourier hologram generation using orthographic projection images," Opt. Express **17**, 6320–6334 (2009).

96. N. Chen, J.-H. Park, and N. Kim, "Parameter analysis of integral Fourier hologram and its resolution enhancement," Opt. Express **18**, 2152–2167 (2010).

97. H. Kim, J. Hahn, and B. Lee, "Mathematical modeling of triangle-mesh-modeled three-dimensional surface objects for digital holography," Appl. Opt. **47**, D117–D127 (2008).

98. F. Zhou, H. B.-L. Duh, and M. Billinghurst, "Trends in augmented reality tracking, interaction and display: a review of ten years of ISMAR," in *Proceedings of 7th IEEE/ACM International Symposium* (IEEE, 2008), pp. 193–202.

99. D. W. F. van Krevelen and R. Poelman, "A survey of augmented reality technologies, applications and limitations," Int. J. Virtual Reality **9**, 1–20 (2010).

100. O. Cakmakci and J. Rolland, "Head-worn displays: a review," J. Disp. Technol. **2**, 199–216 (2006).

101. H. Morishima, T. Akiyama, N. Nanba, and T. Tanaka, "The design of off-axial optical system consisting of aspherical mirrors without rotational symmetry," in *20th Optical Symposium, Extended Abstracts* (Optical Society of Japan, 1995), Vol. 21, pp. 53–56.

102. K. Inoguchi, H. Morishima, N. Nanaba, S. Takeshita, and Y. Yamazaki, "Fabrication and evaluation of HMD optical system consisting of aspherical mirrors without rotation symmetry," in *Japan Optics'95, Extended Abstracts* (Optical Society of Japan, 1995), pp. 19–20.

103. D. Cheng, Y. Wang, H. Hua, and M. M. Talha, "Design of an optical see-through head-mounted display with a low f-number and large field of view using a freeform prism," Appl. Opt. **48**, 2655–2668 (2009).

104. D. Cheng, Y. Wang, H. Hua, and J. Sasian, "Design of a wide-angle, lightweight head-mounted display using freeform optics tiling," Opt. Lett. **36**, 2098–2100 (2011).

105. Z. Zheng, X. Liu, H. Li, and L. Xu, "Design and fabrication of an off-axis see-through head-mounted display with an x–y polynomial surface," Appl. Opt. **49**, 3661–3668 (2010).

106. E. W. Tatham, "Technical opinion: getting the best of both real and virtual worlds," Commun. ACM **42**, 96–98 (1999).

107. O. Cakmakci, Y. Ha, and J. P. Rolland, "A compact optical see-through head-worn display with occlusion support," in *Proceedings of the 3rd IEEE/ACM International Symposium on Mixed and Augmented Reality* (IEEE/ACM, 2004), pp. 16–25.

108. K. Kiyokawa, Y. Kurata, and H. Ohno, "An optical see-through display for mutual occlusion with a real-time stereo vision system," Comput. Graph. Forum **25**, 765–779 (2001).

109. K. Kiyokawa, Y. Kurata, and H. Ohno, "Occlusive optical see-through displays in a collaborative setup," in *Proceedings of the ACM SIGGRAPH* (ACM 2002), p. 74.

110. K. Kiyokawa, M. Billinghurst, S. E. Hayes, A. Gupta, Y. Sannohe, and H. Kato, "Communications behaviors of co-located users in collaborative AR interfaces," in *Proceedings of the IEEE/ACM International Symposium on Mixed and Augmented Reality* (IEEE/ACM 2002), pp. 139–148.

111. K. Kiyokawa, M. Billinghurst, B. Campbell, and E. Woods, "An occlusion-capable optical see-through head mount display for supporting co-located collaboration," in *Proceedings of the 2nd IEEE/ACM International Symposium on Mixed and Augmented Reality* (IEEE/ACM 2003), pp. 133–141.

112. S. Shiwa, K. Omura, and F. Kishino, "Proposal for a 3-D display with accommodative compensation: 3-DDAC," J. Soc. Inf. Disp. **4**, 255–261 (1996).

113. T. Shibata, T. Kawai, K. Ohta, M. Otsuki, N. Miyake, Y. Yoshihara, and T. Iwasaki, "Stereoscopic 3-D display with optical correction for the reduction of the discrepancy between accommodation and convergence," J. Soc. Inf. Disp. **13**, 665–671 (2005).

114. S. C. McQuaide, E. J. Seibel, J. P. Kelly, B. T. Schowengerdt, and T. A. A. Furness, "A retinal scanning display system that produces multiple focal planes with a deformable membrane mirror," Displays **24**, 65–72 (2003).

115. S. Liu, H. Hua, and D. Cheng, "A novel prototype for an optical see-through head-mounted display with addressable focus cues," IEEE Trans. Vis. Comput. Graph. **16**, 381–393 (2010).

116. A. Olwal and T. Höllerer, "POLAR: portable, optical see-through, low-cost augmented reality," in *Proceedings of the ACM Symposium on Virtual Reality Software and Technology* (ACM, 2005), pp. 227–230.

117. W. Wu, F. Blaicher, J. Yang, T. Seder, and D. Cui, "A prototype of landmark-based car navigation using a full-windshield head-up display system," in *Proceedings of the 2009 Workshop on Ambient Media Computing* (ACM 2009), pp. 21–28.

118. A. Sato, I. Kitahara, K. Yoshinari, and O. Yuichi, "Visual navigation system on windshield head-up display," in *Proceedings of 13th World Congress & Exhibition on Intelligent Transport Systems and Services* (Brintex, 2006).

119. K. Palovuori and I. Rakkolainen, "Method and apparatus for forming a projection screen or a projection volume," U.S. patent 6,819,487 (16 November 2004).

120. S. Eitoku, K. Nishimura, T. Tanikawa, and M. Hirose, "Study on design of controllable particle display using water drops suitable for light environment," in *Proceeding of the ACM Symposium on Virtual Reality Software and Technology* (ACM, 2009), pp. 23–26.

121. A. Olwal, S. DiVerdi, N. Candussi, I. Rakkolainen, and T. Höllerer, "An immaterial, dual-sided display system with 3D interaction," in *Proceedings of the IEEE Conference on Virtual Reality* (IEEE, 2006), pp. 279–280.

122. S. DiVerdi, I. Rakkolainen, T. Höllerer, and A. Olwal, "A novel walk-through 3D display," Proc. SPIE **6055**, 605519 (2006).

123. Y. Takaki, Y. Urano, S. Kashiwada, H. Ando, and K. Nakamura, "Super multi-view windshield display for long-distance image information presentation," Opt. Express **19**, 704–716 (2011).

124. Y. Takaki and N. Nago, "Multi-projection of lenticular displays to construct a 256-view super multi-view display," Opt. Express **18**, 8824–8835 (2010).

125. C. Lee, S. DiVerdi, and T. Höllerer, "Depth-fused 3-D imagery on an immaterial display," IEEE Trans. Vis. Comput. Graph. **15**, 20–32 (2009).

126. S. Suyama, Y. Ishigure, H. Takada, K. Nakazawa, J. Hosohata, Y. Takao, and T. Fujikao, "Apparent 3-D image perceived from luminance-modulated two 2-D images displayed at different depths," Vision Res. **44**, 785–793 (2004).

127. Y. Ishigure, S. Suyama, H. Takada, K. Nakazawa, J. Hosohata, Y. Takao, and T. Fujikado, "Evaluation of visual fatigue relative in the viewing of a depth-fused 3D display and 2D display," in *Proceedings of International Display Workshops* (Society for Information Display. 2004), pp. 1627–1630.

128. P. C. Barnum, S. G. Narasimhan, and T. Kanade, "A multi-layered display with water drops," ACM Trans. Graph. **29**, 76 (2010).

129. I. Kasai, Y. Tanijiri, T. Endo, and H. Ueda, "A practical see-through head mounted display using a holographic optical element," Opt. Rev. **8**, 241–244 (2001).

130. A. Olwal, J. Gustafsson, and C. Lindfors, "Spatial augmented reality on industrial CNC-machines," Proc. SPIE **6804**, 680409 (2008).

131. K. Sakamoto, M. Okamoto, H. Ueda, H. Takahashi, and E. Shimizu, "Real-time 3D color display using a holographic optical element," Proc. SPIE **2652**, 124–131 (1996).

132. K. Sakamoto, H. Takahashi, E. Shimizu, H. Ueda, K. Tanaka, and M. Okamoto, "New approach to the real-time 3D display using a holographic optical element," Proc. SPIE **3011**, 36–44 (1997).

133. R. Kishigami, H. Takahashi, and E. Shimizu, "Real-time color three-dimensional display system using holographic optical elements," Proc. SPIE **4296**, 102–107 (2001).

134. H. Takahashi, H. Fujinami, and K. Yamada, "Wide-viewing-angle three-dimensional display system using HOE lens array," Proc. SPIE **6055**, 60551C (2006).

135. J. Hong, Y. Kim, S. Park, J.-H. Hong, S.-W. Min, S.-D. Lee, and B. Lee, "3D/2D convertible projection-type integral imaging using concave half mirror array," Opt. Express **18**, 20628–20637 (2010).